Targeted hydrolysis of native potato protein: A novel route for obtaining hydrolysates with improved interfacial properties

Simon Gregersen Echers[1,*] Ali Jafarpour[2], Betül Yesiltas[2], Pedro J. García-Moreno[2,3], Mathias Greve-Poulsen[4], Dennis Hansen[5], Charlotte Jacobsen[2], Michael Toft Overgaard[1], Egon Bech Hansen[6]

[1] Section for Biotechnology, Department of Chemistry and Bioscience, Aalborg University, Frederik Bajers Vej 7H, 9220 Aalborg, Denmark; sgr@bio.aau.dk (SGE); mto@bio.aau.dk (MTO)

[2] Research Group for Bioactives - Analysis and Application, National Food Institute, Technical University of Denmark, Kemitorvet, 201, Kgs Lyngby, 2800, Denmark; alijaf@food.dtu.dk (AJ); betye@food.dtu.dk (BY); chja@food.dtu.dk (CJ)

[3] Department of Chemical Engineering, University of Granada, Av. de Fuente Nueva, s/n, 18071, Spain; pjgarcia@ugr.es (PJGM)

[4] KMC AmbA, Herningvej, 60, Brande, 7330, Denmark; mgp@kmc.dk (MGP)

[5] Lihme Protein Solutions A/S, Brydehusvej 30L, Ballerup, 2750, Denmark; d.hansen@lps-dk.com (DH)

[6] Research Group for Gut, Microbes and Health, National Food Institute, Technical University of Denmark, Kemitorvet, 202, 1250, Kgs Lyngby, 2800, Denmark; egbh@food.dtu.dk (EBH)

*Corresponding author: sgr@bio.aau.dk (SGE)

Simon Gregersen Echers and Ali Jafarpour contributed equally to this work

Abstract

Peptides and protein hydrolysates are promising alternatives to substitute chemical additives as functional food ingredients. In this study, we present a novel approach for producing a potato protein hydrolysate with improved emulsifying and foaming properties by data-driven, targeted hydrolysis. Based on previous studies, we selected 15 emulsifier peptides derived from abundant potato proteins, which were clustered based on sequence identity. Through *in silico* analysis, we determined that from a range of industrial proteases (Neutrase (Neut), Alcalase (Alc), Flavorzyme (Flav) and Trypsin (Tryp)), Tryp was found more likely to release peptides resembling the target peptides. After applying all proteases individually, hydrolysates were assayed for *in vitro* emulsifying and foaming properties. No direct correlation between degree of hydrolysis and interfacial properties was found. Tryp produced a hydrolysate (DH=5.4%) with the highest ($P<0.05$) emulsifying and foaming abilities, good stabilities, and high aqueous solubility. Using LC-MS/MS, we identified >10,000 peptides in each hydrolysate. Through peptide mapping, we show that random overlapping with known peptide emulsifiers is not sufficient to quantitatively describe hydrolysate functionality. While Neut hydrolysates had the highest proportion of peptides with target overlap, they showed inferior interfacial activity. In contrast, Tryp was able to release specifically targeted peptides, explaining the high surface activity observed. While modest yields and residual unhydrolyzed protein indicate room for process improvement, this work shows that data-driven, targeted hydrolysis is a viable, interdisciplinary approach to facilitate hydrolysis design for production of functional hydrolysates from alternative protein sources.

Keywords: potato protein, targeted hydrolysis, peptide emulsifiers, interfacial properties, quantitative proteomics, peptide identification

1. Introduction

Potato (*Solanum tuberosum*) is the fourth most cultivated crop with a global production of about 370 million tonnes in 2018 (Food and Agriculture Organization of the United Nations, 2020). Potatoes are the second highest protein providing crop per area grown after wheat, and despite a modest protein content of 1-2% depending on cultivar (Camire, Kubow, & Donnelly, 2009; Jørgensen, Stensballe, & Welinder, 2011; Van Koningsveld et al., 2006), they are still regarded as a highly attractive food protein due to both high nutritional quality and functional properties (Waglay & Karboune, 2016b). Potato proteins are often classified according to their cellular function with patatin, also known as tuberin, as the major fraction. Patatins are highly homologous storage proteins with molecular weights (MWs) from 40 to 45 kDa and pIs in the range of 4.8-5.2 (Kärenlampi & White, 2009), which constitute 35-40% of the tuber protein depending on the specific cultivar (Løkra & Strætkvern, 2009). Likewise, protease inhibitors constitute 30–40% of the total tuber protein (Bauw et al., 2006; Jørgensen, Bauw, & Welinder, 2006), but represent a group of more diverse proteins with MWs from 5 to 25 kDa (Heibges, Glaczinski, Ballvora, Salamini, & Gebhardt, 2003; Pouvreau et al., 2001) which can be divided into sub-groups based on sequence homology and thus targets for inhibition (García-Moreno, Gregersen, et al., 2020; Heibges et al., 2003).

Directly isolated from potato fruit juice (PFJ), native potato protein has been reported to exhibit high solubility as well as foaming and emulsifying activity, which has primarily been ascribed to the large patatin content (Ralet & Guéguen, 2000; Schmidt et al., 2019; Van Koningsveld et al., 2001, 2006). To achieve these desirable characteristics, it is important to use appropriate extraction methods to maintain the proteins in their native and intact form, which, from the industrial point of view, would be costly. Thus, the industrially isolated potato protein, mainly obtained in

71 denatured form through rather harsh heat coagulation and acid precipitation, lacks those above-
72 mentioned functionalities. However, due to high content of amino acids with hydrophobic
73 functional groups, in particular, with branched (isoleucine, leucine, and valine) and aromatic
74 (phenylalanine and tyrosine) side chains (Refstie & Tiekstra, 2003), techno-functionality of potato
75 protein can potentially be improved when the large, denatured proteins undergo a specific set of
76 hydrolysis steps to yield smaller peptides (Aluko, 2018; Li-Chan, 2015; Moreno, Cuadrado,
77 Marquez Moreno, & Fernandez Cuadrado, 1993; Rodan, Fields, & Falla, 2013; Wang & Xiong,
78 2005). Enzymatically released peptides may display better functional properties than their parent
79 protein molecules and consequently exhibit higher activity in food systems (Kamnerdpetch, Weiss,
80 Kasper, & Scheper, 2007; Moreno et al., 1993). Moreover, potato protein hydrolysates have also
81 been shown to have beneficial health effects *in vivo* (Chuang et al., 2020), illustrating their
82 potential as both a functional and bioactive ingredients.
83 Amphiphilic surfactants are widely used as emulsifiers as they contain both hydrophobic and
84 hydrophilic regions, which are capable of reorganising at the oil-water interface and thereby
85 stabilize the emulsion by decreasing the interfacial tension between the two immiscible liquids
86 (McClements & Jafari, 2018). In this respect, the use of peptides as natural emulsifiers and
87 biosurfactants has received increasing attention over the past few decades from both the academic
88 and the industrial sector (Adjonu, Doran, Torley, & Agboola, 2014; Dexter & Middelberg, 2008;
89 Hanley & James, 2018; Le Guenic, Chaveriat, Lequart, Joly, & Martin, 2019). Peptides are
90 complex polymer chains combining (at least) twenty different amino acid monomers with different
91 physico-chemical properties and thus, the combinatorial space is tremendous and scales by peptide
92 length, n, as (at least) 20^n. Although the specific mechanisms and prerequisites for potent peptide
93 emulsifiers still remains only superficially characterized, our understanding of the underlying

molecular properties continue to expand (Ricardo, Pradilla, Cruz, & Alvarez, 2021). Recent work has investigated the influence of factors such as interfacial peptide structure (Dexter, 2010; Du et al., 2020; García-Moreno et al., 2021; Lacou, Léonil, & Gagnaire, 2016), physico-chemical properties such as length and charge (García-Moreno, Gregersen, et al., 2020; Lacou et al., 2016; Liang et al., 2020; Yesiltas et al., 2021), amino acid composition (Enser, Bloomberg, Brock, & Clark, 1990; Saito, Ogasawara, Chikuni, & Shimizu, 1995; Siebert, 2001), and specific sequence patterns (Jafarpour, Gregersen, et al., 2020; Mondal et al., 2017; Nakai et al., 2004; Wychowaniec et al., 2020). Although various factors do appear to influence emulsification, the potential appears to indeed depend significantly on the propensity of a given peptide to adopt a more well-defined amphiphilic structure at the interface (Dexter & Middelberg, 2008; Enser et al., 1990; Saito et al., 1995). This property, in turn, is governed by these underlying factors. Although not appearing to be governed by the exact same molecular mechanisms, the stabilization of the air-water interface in foams have been suggested to also depend on peptide amphiphilicity (Enser et al., 1990; Jafarpour, Gregersen, et al., 2020).

Consequently, identification and molecular characterization of isolated peptides could enhance the understanding of functional mechanism and potential of enzymatic protein hydrolysates in food systems, such as emulsions and foams. Moreover, it would allow for development of targeted processes for release of specific peptides with known functional properties. This, in turn, could result in improved modification of a potato by-product to generate more value added ingredients with promising beneficial properties (Karami & Akbari-adergani, 2019). Waglay and Karboune, (2016a) characterized the structure of enzymatically generated peptides from potato protein, however, these authors did not correlate the specified characterization with functionality properties (Waglay & Karboune, 2016a). García-Moreno et al. (2020) investigated the emulsifying activity

of six potato peptides (23–29 amino acids) predicted by bioinformatics as having potentially different predominant structure at the oil/water interface (e.g. α-helix, β-strand or unordered). The authors found that γ-peptides (half-hydrophobic and half-hydrophilic peptides with axial amphiphilicity), showed higher emulsifying activity, compared to α-helix and β-strand peptides, in agreement with their predictions (García-Moreno, Jacobsen, et al., 2020). However, generalization is not possible on such limited data. The study was followed by a more elaborate investigation of potato protein derived emulsifier peptides (García-Moreno, Gregersen, et al., 2020), showing that this could indeed not be generalized. In fact, the most promising peptide emulsifier (γ1) was later shown to adopt a predominantly α-helical conformation at the interface, thereby possessing both axial and facial amphiphilicity (García-Moreno et al., 2021). Although the structure-function relationship of emulsifier peptides from potato protein is more complex than predictable secondary structure and amphiphilicity, the two factors can be regarded as good indicators of emulsification potential (García-Moreno, Gregersen, et al., 2020).

Until now, most studies on protein hydrolysates are conducted using a trial-and error approach, where various industrial proteases are used to digest proteins in an untargeted manner. In such studies, process parameters (e.g. protease selection, pH, temperature, protein concentration, enzyme/substrate ratio, and time) are usually optimised in respect to bulk hydrolysate characteristics such as yield or functionality, with little or no attention to peptide-level insight. The application of mass spectrometry has in these instances mainly been focused on identification of peptides with high intensities in the bulk hydrolysate or in the high activity fractions. While such analysis may provide insight on peptides potentially responsible for the observed bulk functionality, it does not provide sufficient evidence unless functional properties are validated for the isolated peptide. In this study, we present the fundamentally different approach of data-driven,

140 targeted hydrolysis. Building on existing knowledge on potato protein-derived peptide emulsifiers,
141 we present a workflow where *in silico* sequence analysis is used as a guide for protease selection.
142 By prediction of peptide release based on protease specificity, we hypothesise that application of
143 specific proteases should produce a hydrolysate with better surface active (i.e. emulsifying and
144 potentially foaming) properties. The approach is benchmarked against a range of commonly used
145 industrial proteases, and the hydrolysates are characterised for their bulk physico-chemical and
146 functional properties with particular focus on emulsification of fish oil and foam formation.
147 Ultimately, we apply mass spectrometry-based proteomics analysis to qualitatively and
148 quantitatively characterize the peptidome of the hydrolysates and relate these findings to both *in*
149 *vitro* functionalities, predicted peptide release, and *a priori* knowledge on potato peptide
150 emulsifiers. With this approach, we showcase how proteomics and bioinformatics may lay the
151 basis for targeted process design in the future of peptide-based functional food ingredient
152 development and production.
153

154 ## 2. Materials and methods

155 Potato protein isolate (PPI) (87% protein, determined by Kjeldal-N and Dumas) was supplied by
156 KMC AmbA (Brande, Denmark). The PPI was obtained using a proprietary, cold extraction
157 method yielding native, non-denatured proteins. Alcalase 2.4L (2.4 AU/g), Neutrase 0.8L (0.8
158 AU/g), Flavorzyme 1000 L (1000 LAPU/g), and Trypsin (Pancreatic Trypsin Novo (PTN) 6.0S
159 (6.0 AU/g) were provided by Novozymes A/S, (Bagsværd, Denmark). Distilled deionized water
160 was used for the preparation of all solutions during hydrolysate production. As reference for
161 emulsification experiments, sodium caseinate (SC) and purified, native patatin was used. SC
162 (Miprodan 30) was supplied by Arla Foods Ingredients AmbA (Viby J, Denmark) and patatin was

purified from the PPI by Lihme Protein Solutions (Kongens Lyngby, Denmark) using a gentle, sequential precipitation through a proprietary pH-shift methodology. All chemicals used were of analytical grade.

2.1.Target peptide selection, in silico sequence analysis, and process design for targeted hydrolysis

Previously investigated peptides derived from potato proteins were evaluated for emulsification potential based on published data (García-Moreno, Gregersen, et al., 2020; García-Moreno, Jacobsen, et al., 2020; García-Moreno et al., 2021; Yesiltas et al., 2021). Peptides were categorized (Table A.1) on a three-level scale (high (1), intermediate (2), and low (3)) according to their ability to i) reduce oil/water interfacial tension (IFT), ii) decrease oil droplet size, and iii) lead to physically stable emulsions during storage in comparison to SC. For IFT, peptides were evaluated based on their IFT at 30 min and classified as high if IFT < 15 mN/m, intermediated if 15 mN/m < IFT < 20 mN/m, and low if IFT > 20 mN/m (IFT for SC was reported as 10-14 mN/m in the four studies). For oil droplet size, peptides were evaluated by their mean diameter after emulsion (5% fish oil in water stabilized by 0.2% (W/V) peptide) production, either by $D_{4,3}$ or $D_{3,2}$ depending on what was reported in the individual studies. Peptides were classified as high if $D < D_{SC}$, intermediate if $D_{SC} < D < 3x\ D_{SC}$, and low if $D > 3x\ D_{SC}$. For physical stability, peptides were classified as high if D did not increase by more than 100% after storage (compared to itself and/or SC) and no or little creaming was observed, intermediate if D did not increase by more than 300% after storage (compared to itself and/or SC) and middle/high creaming was observed, and low if D increased more than 300% after storage (compared to itself and/or SC) and/or severe creaming or separation was observed.

Peptide classified as high or intermediate in all three categories were selected for further *in silico* sequence analysis and ranked by their mean score across the three categories (and different studies, where applicable). To investigate potential release by enzymatic hydrolysis using the available proteases, the specific peptide was localized in the protein of origin (according to the original study) and the region of the protein containing the peptide and 15 amino acids up- and downstream (Table 1) extracted from Uniprot (Consortium et al., 2021). Cleavage specificity of the proteases was used to manually analyze potential hydrolysis of the protein region, where Tryp specificity is well-established and cleaves after Lys/Arg (K/R). Alc and Neut are broad specificity proteases but supplier specificity (Novozymes A/S) was used for *in* silico analysis. As such, Alc has a strong preference to cleave after Leu/Phe/Tyr/Gln (L/F/Y/Q), while Neut shows preference to cleave before Leu/Ile/Phe/Val (L/I/F/V). Flav is a complex mixture of endo- and exoproteases (Rabe et al., 2015), and cleavage specificity has not been established. As such, Flav was used merely as a reference protease due to its widespread use in the food industry. Based on distribution of target amino acids in and around the peptides, application of the individual proteases was evaluated, and the best possible process determined. To validate the approach and benchmark the method of targeted hydrolysis, all proteases were applied experimentally.

2.2.Potato protein hydrolysate preparation

Potato protein hydrolysates (PPHs) were produced from a native PPI, using two enzymatic hydrolysis strategies; (A) free-fall pH hydrolysis of native PPI, and (B) free-fall pH mode with protein heat denaturation prior to hydrolysis. In method A, a 1% (w/v) protein solution was prepared by gradual addition of PPI to distilled water and solubilized for 15 min by magnetic stirring. In method B, a 10% (w/v) PPI solution was prepared, heated to 90°C for 30 min, and

209 resulting slurry was diluted 1:1 with distilled water to a final protein concentration of 4.35% (w/v).
210 The pH of all PPI solutions was adjusted to 8.0 by 1M NaOH followed by addition of protease
211 (Alcalase (Alc), Neutrase (Neut), or Flavourzyme (Flav), and Trypsin (Tryp)) at varying
212 enzyme/substrate (E/S) ratio. For method A, E/S ratios of 0.1%, 0.5%, and 1% were applied while
213 for method B, E/S ratios of 0.1% 1%, and 3% were applied. In both methods, hydrolysis was
214 carried out at 50°C for 2 h. pH and temperature was selected to accommodate activity ranges of
215 all proteases according to manufacturer (Novozymes A/S supplied information).
216 Following hydrolysis, the pH of the solution was adjusted to 7.0 with either 1M NaOH or 1M HCl
217 and supernatants were heated to 90 °C for 15 min for enzyme inactivation. After cooling by tap
218 water, solutions were centrifuged at 10,000 ×g for 20 min at 20 °C and the supernatant collected.
219 The PPH was lyophilized and stored at 4 °C until further analysis. The two applied hydrolysis
220 strategies are illustrated in Fig. 1.
221

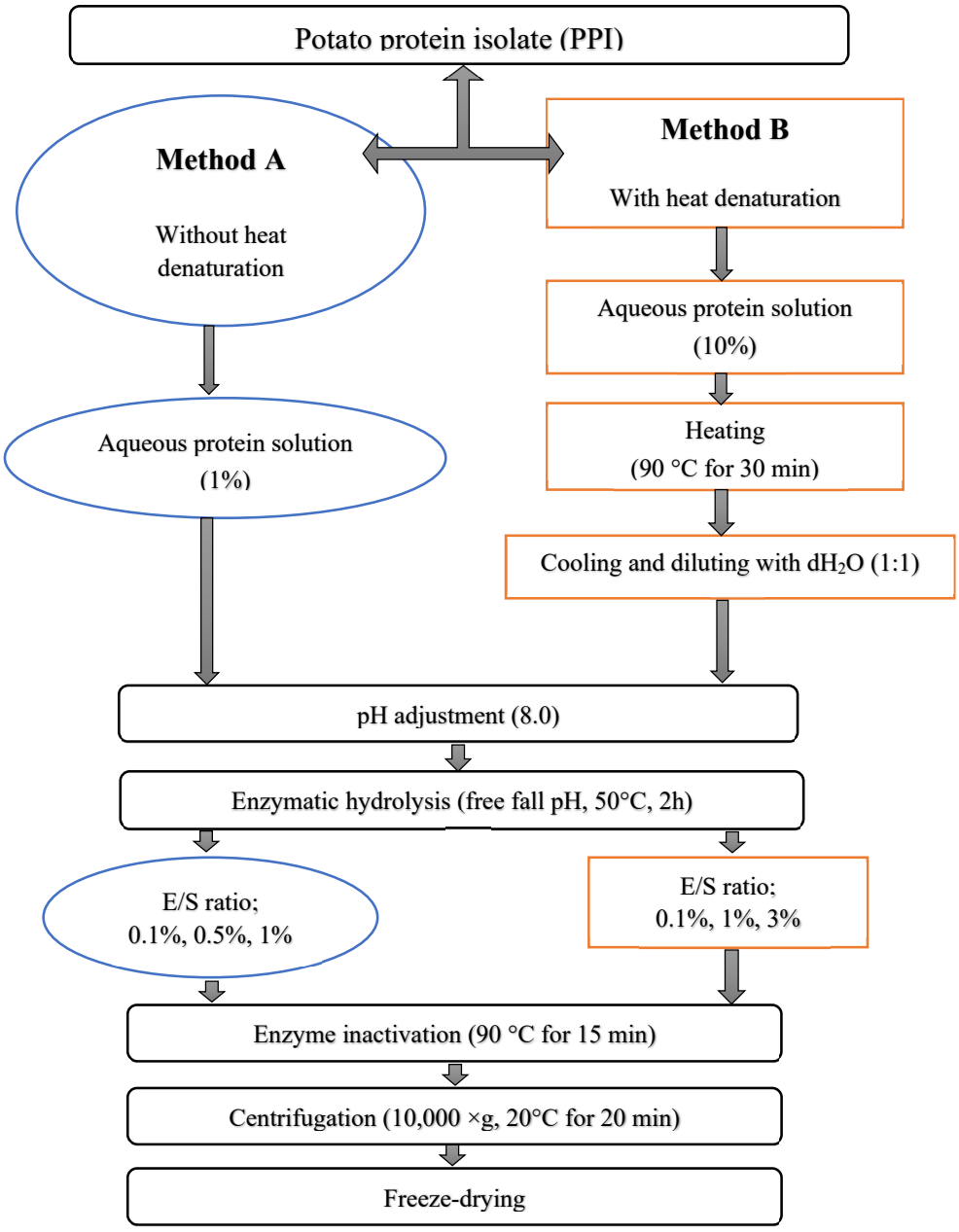

Fig. 1: Flow chart for the enzymatic hydrolysis of potato protein isolate (PPI) by application of Alc, Neut, Flav or Tryp using two different processes; (A, left) without heat denaturation of PPI and (B, right) with heat denaturation to inactivate protease inhibitors. Steps specific for method A are depicted in circles while steps specific for method B are depicted in squares. Common steps are depicted as rounded squares spanning both workflows.

2.3.Degree of hydrolysis and peptide chain length

Degree of hydrolysis (DH) was determined based on α-amino nitrogen content as previously described (Jafarpour, Gregersen, et al., 2020) with minor modifications, adjusting for the α-amino nitrogen content of the untreated substrate. Briefly, free α-amino content of PPHs was determined using the PFAN-25 free amino nitrogen assay kit (PractiChrom, USA) measured using A_{530} on a Picoexplorer (USHIO INC, USA), according to manufacturer guidelines, using glycine as reference for standard curve generation. DH was calculated as:

$$DH\% = \frac{AN_i - AN_0}{AN_{tot} - AN_0} \times 100$$

where AN_i is the concentration of α-amino nitrogen (mM/g substrate) resulting from hydrolysis at a given time, i, AN_0 is the α-amino nitrogen content of the untreated substrate, and AN_{tot} is the total amount of α-amino nitrogen content following complete hydrolysis with 6 M HCl at 110°C for 24 h, as previously described (Jafarpour, Gomes, et al., 2020). AN_{tot} was based on duplicate amino acid (AA) analysis and calculated using the molecular weight of individual AAs. All determinations of α-amino-N were performed in triplicates.

The determined DH for the individual PPHs was used to estimate the average peptide chain length (PCL_{DH}) as:

$$PCL_{DH} = \frac{1}{DH(\%)} * 100$$

250 *2.4.Nitrogen recovery and protein content*

251 Total nitrogen content was determined using the Dumas combustion method using a fully
252 automated Rapid MAX N (Elementar Analysensysteme GmbH, Langenselbold, Germany), and
253 nitrogen recovery (NR) in the soluble fraction was determined as previously reported (Jafarpour,
254 Gomes, et al., 2020) and calculated as:

255

256 $$NR\ (\%) = \frac{N_{PPH} \times\ m_{PPH}}{N_i\ \times m_i} \times 100\%$$

257

258 where N_{PPH} is nitrogen content (%) in the PPH, m_{PPH} is the mass (g) of analysed PPH, N_i is the
259 nitrogen content (%) of the initial substrate, and m_i is the mass (g) of the initial substrate analyzed.
260 Prior to analysis, the system was calibrated using multiple blanks, aspartic acid, and wheat protein
261 isolates. The protein content was estimated using a standard industrial nitrogen to protein
262 conversion factor of 6.25 (Jones, 1931; Mariotti, Tomé, & Mirand, 2008)

263

264 *2.5.Yield*

265 The yield of hydrolysis was determined as the mass ratio to the initial substrate mass, as

266

267 $$Yield\ (\%) = \frac{m_{PPH}}{m_i} \times 100\%$$

268

269 where m_{PPH} is the mass (g) of obtained PPH after lyophilization and m_i is the mass (g) of initial
270 substrate.

271

2.6.PPH solubility

The relative solubility at 10 mg/mL of PPI/PPHs was determined based on nitrogen content by Dumas, as previously described (Jafarpour, Gomes, et al., 2020). Briefly, 200 mg PPH was dissolved in 20 mL of 0.1 M sodium phosphate buffer (pH=7.4), vortexed for 10 s, shaken at 80 rpm for 30 min, and centrifuged at 7500 ×g for 15 min. PPH solubility was calculated as:

$$Solubility\ (\%) = \frac{P_{sup}}{P_{tot}} \times 100\%$$

where P_{sup} is protein/peptide content in supernatant and P_{tot} is total protein/peptide content in PPI the respective PPH as obtained for determination of NR. Measurements were performed in triplicate.

2.7.Bulk Density

The bulk density of the PPHs was determined according to (Jafarpour, Gomes, et al., 2020). Briefly, 5g PPH was added to a 50 mL graduated cylinders and gently tapped 10 times on the lab bench. Bulk density was reported as g/mL.

2.8.Color parameters

The tristimulus color parameters ($L^*a^*b^*$) of PPHs were recorded using a Miniscan XE colorimeter (Hunter Lab, Reston, Virginia, USA) and the whiteness of PPHs was determined in accordance with (Hashemi & Jafarpour, 2016) and calculated as:

294 $$W = 100 - \sqrt[2]{(100 - L^*)^2 + a^{*2} + b^{*2}}$$

295

296 Where, *W* is whiteness index, *L**; indicating lightness from black (0) to white (100); *a**; indicating
297 redness from green (- 120) to red (+120); and *b**; indicating yellowness going from blue (-120) to
298 yellow (+120). Measurements were performed in triplicate.

299

300 *2.9.Emulsifying properties*

301 Emulsifying activity index (EAI) and emulsion stability index (ESI) were determined using the
302 method described by (Pearce & Kinsella, 1978) with slight modifications, previously described
303 (Jafarpour, Gregersen, et al., 2020). Briefly, 15 mL PPH in distilled water (2 mg/mL) was mixed
304 with 5 mL rapeseed oil by an ultraturax homogenizer (IKA, Germany) at speed of 9,500 rpm for
305 60 s without pH adjustment. Fifty µL aliquots were pipetted from the bottom of the container at 0
306 and 10 min after homogenization and added to 5 mL of 0.1% sodium dodecyl sulfate (SDS)
307 solution and mixed by gentle shaking. The absorbance of the diluted solution was measured at 500
308 nm using a spectrophotometer (SHIMADSU UV-1280, Japan). EAI was calculated as:

309

310 $$EAI\left(\frac{m^2}{g}\right) = \frac{2 \times 2.303 \times A_0 \times D}{\emptyset \times c \times 10{,}000}$$

311

312 where A_0 is the absorbance at 500nm immediately following homogenization, *D* is dilution factor
313 (100), $\emptyset$ is oil volume fraction (0.25) and *c* is protein concentration (g/mL).
314 ESI was calculated as:

315

316 $$ESI(min) = \frac{A_0 \times \Delta T}{\Delta A}$$

317

318 where ΔT is equal to 10 min and ΔA is the difference in absorbance at 500 nm after 0 and 10 min
319 ($\Delta A = A_0 - A_{10}$). Enriched patatin, untreated PPI, and SC solutions (2mg/mL) were used as
320 references. Measurements were performed in triplicates.

321

322 *2.10. Foaming properties*

323 Foaming capacity (FC) and foaming stability (FS) were determined according to the method of
324 (Elavarasan, Naveen Kumar, & Shamasundar, 2014) and calculated as previously described
325 (Jafarpour, Gregersen, et al., 2020). Accordingly, 0.1 % (w/v) PPH in distilled water was
326 homogenized at 9,500 rpm for 120 s using an Ultraturrax (IKA, Germany), and poured into a 200
327 mL graduated cylinder. FC was calculated as:

328

329 $$FC(\%) = \frac{V^0_{foam}}{V_{init}} \times 100\%$$

330

331 where V^0_{foam} is the foam volume immediately after homogenization and V_{init} is the initial sample
332 volume.
333 FS was determined after a 30 min resting period (FS_{30}) and calculated as:

334

335 $$FS_{30}(\%) = \frac{V^{30}_{foam}}{V^0_{foam}} \times 100\%$$

336

where V^{30}_{foam} is the foam volume after 30 min. Measurements were performed in triplicates.

2.11. 1D SDS-PAGE analysis

For visualization of the hydrolysis using both strategies, PPHs were analyzed by SDS-PAGE. using SurePAGE 4-20% gradient Bis-Tris gels (Genscript, Picastaway, NJ, USA) under reducing conditions, as previously described (Jafarpour, Gregersen, et al., 2020). As controls, the unhydrolyzed PPI sample and a process control (PPI with no added protease but same treatment) were included.

2.12. Peptide analysis by LC-MS/MS

Lyophilized PPH was solubilized in a detergent-containing buffer, reduced and alkylated in-solution, and desalted using C-18 StageTips, and dried by SpeedVac, as previously described (Jafarpour, Gomes, et al., 2020). Desalted peptides were solubilized in solvent A (0.1% aq. formic acid (FA)) and 1µg (determined by NanoDrop (Thermo Scientific Bremen, Germany)) was loaded and separated on an EASY-nLC (Thermo Scientific) equipped with a reverse phase (RP) Acclaim Pepmap Nanotrap column (C18, 100 Å, 100 µm.×2 cm, nanoViper fittings (Thermo Scientific)) followed by a RP Acclaim Pepmap RSLC analytical column (C18, 100 Å, 75 µm.×50 cm, nanoViper fittings (Thermo Scientific). Eluted peptides were introduced into a Q Exactive HF mass spectrometer (Thermo Scientific) via a Nanospray Flex ion source (Thermo Scientific) using a fused silica needle emitter (New Objective, Woburn, MA, USA). Samples were loaded at 8 µL/min and eluted by constant flow at 300 nL/min during a 120 min ramped gradient, ranging from 5 to 100% of solvent B (0.1% formic acid (FA), 80% (V/V) acetonitrile). MS data was

359 acquired in positive mode using a Top-20 data-dependent method. Survey scans were acquired
360 from 200 m/z to 3,000 m/z at a resolution of 60,000 at 200 m/z and the HCD fragmentation spectra
361 were acquired at a resolution of 30,000 at 200 m/z using an isolation window of 1.2 m/z and a
362 dynamic exclusion window of 30 s. The maximum ion injection time was set to 150 ms for both
363 MS and MS/MS scans. ACG target was set to 3e6 and 2e5 for MS and MS/MS scans, respectively.
364 Charge exclusion was only applied for unassigned isotope peaks (all charge states allowed).
365 Peptide match and exclude isotopes were enabled.
366

367 ### *2.13. LC-MS/MS data analysis in MaxQuant*

368 MS raw data was analyzed in MaxQuant v.1.6.10.43 (Cox & Mann, 2008; Tyanova, Temu, & Cox,
369 2016), as previously described (Jafarpour, Gomes, et al., 2020). Briefly, unspecific *in silico*
370 digestion was employed to identify peptides in the range 3-65 AAs. Data was searched against a
371 manually curated version of the full protein database for *Solanum tuberosum* (tax:4113) from
372 UniProt (Consortium et al., 2021) where redundant fragments were removed, as previously
373 described (García-Moreno, Gregersen, et al., 2020). Standard settings were applied, using a 5%
374 false discovery rate (FDR) on both peptide and protein level (Gregersen et al., 2022), including
375 reverse sequences for FDR control, and including common contaminants.
376

377 ### *2.14. Summary statistics and mean peptide properties*

378 Following removal of false positives and contaminants, Venn diagrams were created to visualize
379 peptide identifications and similarity between PPHs. Peptide tables were treated according to the
380 intensity-weighted peptide abundance estimation methodology, as previously described

(Jafarpour, Gomes, et al., 2020; Jafarpour, Gregersen, et al., 2020), and average peptide length (PCL_{avg}) was calculated as:

$$PCL_{avg} = \frac{\sum_{p=1}^{n} PCL_p * I_p}{\sum_{p=1}^{n} I_p}$$

where PCL_p is the length of peptide p of n identified and quantified peptides and I_p is the MS1 intensity of the same peptide.

2.15. Qualitative and quantitative correlation with known potato peptide emulsifiers

For correlation of identified peptides with known emulsifier peptides derived from potato proteins, a set of seven selected target clusters were constructed (Table 1). Here, single AA substitutions were disregarded. For each cluster, a representative cluster sequence spanning the entire sequence with "X" representing variable residues (i.e. AAs where substitutions occur within the cluster peptides) was created. All peptides related to the class/family of proteins associated with the cluster were initially included and subjected to filtering based on two criteria. To be regarded as a potentially emulsifying peptide contributing to the bulk activity observed, the identified peptides were >12 AAs in length, which was previously identified as the minimum length to have emulsifying properties (García-Moreno, Gregersen, et al., 2020; Yesiltas et al., 2021). In addition, a sequence overlap of any peptide of >50% with the representative cluster sequence was required. To facilitate this, all lead proteins (i.e. the first protein in the protein group constructed in MaxQuant) within a relevant class/family of proteins (i.e. patatins and all protease inhibitors) were aligned using Clustal Omega (Sievers et al., 2011). Aligned proteins within each class/family were

grouped into protein sequence clusters where a specific target cluster sequence was represented. Within each protein sequence cluster, sequence identity was not required but AA numbers were aligned. Sequence overlap between identified peptides and a representative cluster sequence was determined through the following set of equations:

$$if\ P_E < C_S \longrightarrow overlap = 0$$

$$if\ P_S > C_E \longrightarrow overlap = 0$$

$$if\ P_S < C_S\ \&\ P_E \leq C_E \longrightarrow overlap = \frac{1 + P_E - C_S}{L}$$

$$if\ P_S < C_S\ \&\ P_E > C_E \longrightarrow overlap = \frac{1 + C_E - C_S}{L}$$

$$if\ P_S \geq C_S\ \&\ P_E \leq C_E \longrightarrow overlap = 1$$

$$if\ P_S \geq C_S\ \&\ P_E > C_E \longrightarrow overlap = \frac{1 + C_E - P_S}{L}$$

where P_S and P_E are the AA positions for the start and end of an identified peptide when mapped to a certain protein cluster sequence, C_S and C_E are the AA positions for the start and end of a representative cluster sequence when mapped to the same protein cluster sequence, L is the length of the identified peptide. Peptides were classified as >50%, >75%, and >95% overlap, thereby with increasing confidence of emulsifier activity with increasing sequence overlap. The five most abundant (by MS1 intensity) peptides from each PPH with >50% overlap with representative cluster sequence were extracted and mapped to the representative cluster sequence using the NCBI blastp suite. The alignment was then visualized in the NCBI multiple sequence alignment (MSA) viewer using the built-in hydropathy color scale and with substitutions indicated.

2.16. Protein-level quantitative distribution of PPH peptides

To determine the protein-level distribution of peptides in PPHs, the method of unspecific, length-normalized relative intensity, I_L^{rel} , was used (Gregersen et al., 2021, 2022). In short, the relative molar abundance of an identified protein (group) was estimated as:

$$I_{rel}^{L}(n) = \frac{I_n / L_n}{\sum_{n=1}^{p} I_n / L_n} * 100\%$$

where I_n is the intensity of protein n (i.e. sum of all peptide intensities ascribed to the protein (group)) of p quantified proteins in a given PPH and L_n is the length of protein n. Subsequently, proteins were grouped according to family/class (García-Moreno, Gregersen, et al., 2020), and the relative abundance of each class was determined.

2.17. Statistical Analysis

The statistical significance between measurements was determined by variance analysis (ANOVA) using Statgraphics software (version 18.1.06 for Windows), and means were compared by Duncan's multiple comparison post-test. Statistical differences were considered to be significant at $p < 0.05$.

3. Results and Discussion

3.1.In silico analysis and design of a targeted hydrolysis process

Based on previously published data on *in vitro* emulsifying properties of potato protein-derived peptides, 58 peptides were evaluated and ranked by their ability to reduce oil/water interfacial tension, mean droplet size after emulsification of 5% fish oil in water, and physical stability of the emulsion (Table A.1). From the initial evaluation, 15 unique peptides with strong emulsifying properties were selected for further *in silico* analysis to identify release potential by enzymatic hydrolysis (Table 1). The 15 selected peptides group into seven clusters by sequence similarity, where particularly cluster 1 is densely populated. Here it is evident that cluster peptides are all related to γ1, being either truncated variants or truncated isoforms of the peptide.

Table 1: Cluster representation of final target peptides listing the peptides annotation from the reference study (Ref) along with the Uniprot identifier (AC#), protein name, sequence window (target peptide **(in bold)** along with the N- and C-terminal 15 amino acids cleavage window for *in silico* sequence and release analysis), average score (see Table A.1), and the cluster number (based on sequence overlap in identical or isoform proteins). Below each cluster, the aligned cluster consensus sequence is indicated with variable residues depicted as *"X" in italics*.

Pep	AC#	Protein	Sequence window	Score	Ref.*	Cluster
γ1	P15477	Patatin-B2	AKLEEMVTVLSIDGG**GIKGIIPAIILEFLEGQLQEVDNNKDAR**LADYFDVIGGTSTGG	1.0	a,b,d	
γ104	Q3YJT3	Pat-2-Kuras 1	GEMVTVLSIDGGGIK**GIIPATILEFLEGQLQEVDNNKDAR**LADYFDVIGGTSTGG	1.0	c	
γ105	Q3YJT4	Pat-1-Kuras 2	EEMVTVLSIDGGGIK**GIIPGTILEFLEGQLQK**MDNNADARLADYFDV	1.0	c	
γ48	Q3YJT3	Pat-2-Kuras 1	GEMVTVLSIDGGGIK**GIIPATILEFLEGQLQEVDNN**KDARLADYFDVIGGT	1.3	b	1
γ75	P15477	Patatin-B2	EEMVTVLSIDGGGIK**GIIPAIILEFLEGQLQEVDNNKDAR**LADYFDVIGGTSTGG	1.3	d	
γ76	P15477	Patatin-B2	EEMVTVLSIDGGGIK**GIIPAIILEFLEGQLQEVDNNK**DARLADYFDVIGGTS	1.3	d	
	Consensus		GIKGIIP*XX*ILEFLEGQLQ*X*VDNNKDAR			
γ40	Q3S474	KTI-B	NLLYCPVTSTMICPF**SSDDQFCLKVGVV**HQNGKRRLALVKDNP	1.2	b,d	
β22	Q3S474	KTI-B	LGYNLLYCPVTSTMI**CPFSSDDQFCLKVGV**VHQNGKRRLALVKDN	1.8	b,d	2
	Consensus		CPFSSDDQFCLKVGVV			
α12	P15477	Patatin-B2	LVQVGETLLKKPVSK**DSPETYEEALKRFAKLLSD**RKKLRANKASH**	1.3	b,d	
α10	P15477	Patatin-B2	EANMELLVQVGETLL**KKPVSKDSPETYEEALKRFAKLLSDRKKL**RANKASH**	1.7	b,d	3
	Consensus		KKPVSKDSPETYEEALKRFAKLLSDRKKL			
γ36	Q3YJT3	Pat-2-Kuras 1	LQEVDNNKDARLADY**FDVIGGTSTGGLLTAMITTPNENNRP**FAAAKDIVPFYFEHG	1.3	b,d	4
	Consensus		FDVIGGTSTGGLLTAMITTPNENNRP			
β27	Q3S488	KTI-A	VRFIPLSTNIFEDQL**LNIQFNIPTPKLC**VSYTIWKVGNINAPLR	1.5	b,d	5
	Consensus		LNIQFNIPTPKLC			
γ38	Q3S474	KTI-B	PVTSTMICPFSSDDQ**FCLKVGVVHQNGKRRLALVKDNP**LDVSFKQVQ**	1.7	b,d	
γ49	Q3S477	KTI-B	YCPATMICPFCSDDE**FCLKVGVIHQNGKRRLALVK**DNPLDVSFKQVQ**	2.0	b	6
	Consensus		FCLKVGV*X*HQNGKRRLALVKDNP			
α2	P15477	Patatin-B2	DICYSTAAAPIYFPP**HHFVTHTSNGARYEFNLVDGAVATVGDPA**LLSLSVATRLAQEDP	2.0	a	7
	Consensus		HHFVTHTSNGARYEFNLVDGAVATVGDPA			

* References: a (García-Moreno, Jacobsen, et al., 2020), b (García-Moreno, Gregersen, et al., 2020), c (Yesiltas et al., 2021), and d (García-Moreno et al., 2021). ** End of protein sequence

453 Alc has broad specificity and has been reported to cleave after a wide range of residues
454 (Ala/Leu/Val/Phe/Tyr/Trp/Glu/Met/Ser/Lys) with varying claims throughout literature (Doucet,
455 Otter, Gauthier, & Foegeding, 2003; Lei, Cui, Zhao, Sun-Waterhouse, & Zhao, 2014; Lu et al.,
456 2021; Sbroggio, Montilha, Figueiredo, Georgetti, & Kurozawa, 2016). A similar lack of consensus
457 for Neut specificity is also found, although varying reports on the broad specificity of Alc and
458 Neut exist, an *in silico* analysis based on supplier specificity (Novozymes A/S) was performed.
459 Using the target peptide sequence and including a 15 amino acid N- and C-terminal cleavage
460 window, all cleavage sites of Alc, Neut, and Tryp were mapped (Fig. 2).
461

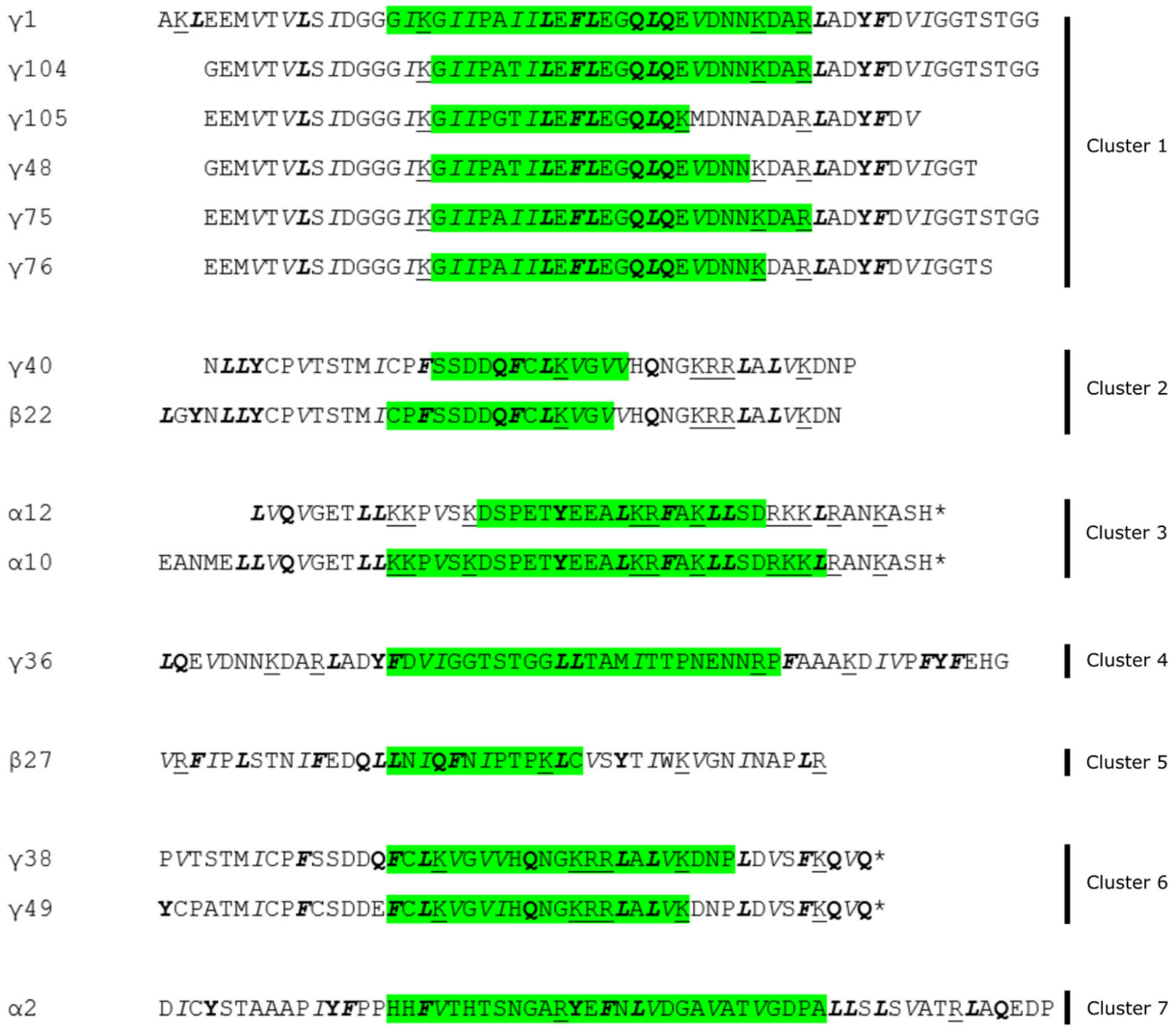

462

463 **Fig. 2**: *In silico* analysis of release potential for selected target peptides following enzymatic hydrolysis by
464 Tryp, Alc, or Neut. Peptides with validated *in vitro* emulsifying properties (highlighted in green) are listed
465 with a 15 amino acid N- and C-terminal cleavage window and clustered by sequence similarity (Table 1).
466 Cleavage sites for Tryp (cleavage after R/K) are underlined, cleavage sites for Alc (cleavage after L/F/Y/Q)
467 are highlighted in **bold**, and cleavage sites for Neut (cleavage before I/L/F/V) are highlighted in *italics*. Alc
468 and Neut both cleave at Phe (F) and Leu (L). "*" indicates the end (C-terminus) of the native protein
469 sequence.

470

In cluster 1, a good overall compatibility with tryptic cleavage is observed. Tryp hydrolysis will result in a three AA N-terminal truncation of γ1 (resulting in γ75) and a three AA C-terminal truncation of γ75 (resulting in γ76). As the C-terminal Lys in γ76 is followed by an Asp, cleavage efficiency for Tryp may be reduced in this position (Giansanti, Tsiatsiani, Low, & Heck, 2016), making γ75 the most probable product, as previously reported (García-Moreno, Gregersen, et al., 2020; García-Moreno et al., 2021). While γ48, γ105, and γ106 originate from other isoforms of patatin and thus contains different AA substitutions, placement of tryptic AAs are highly favourable as well. Target AAs for both Alc and Neut are abundant within all cluster 1 peptides making release of the peptides less likely. Nevertheless, target AAs for Neut are located favourably in both termini of cluster 1 peptides, and some release of highly related peptides may be possible if excessive internal hydrolysis is avoided, although this is considered unexpected in a controlled and reproducible manner.

In cluster 2, target AAs for Tryp are unfavourably distributed. Similarly to cluster 1, target AA for both Alc and Neut are abundant in both peptides, although partial hydrolysis could release peptides very similar to the targets for both proteases. In cluster 3, α12 is fully embedded in α10. Nevertheless, both peptides have centrally located target AAs of all three proteases, making them unlikely products of hydrolysis. However, placement of AAs in the terminal regions may make them decent targets for partial hydrolysis by all three proteases. Cluster 4 contains a single peptide (γ36) and is found in the region of patatin immediately following cluster 1. Hydrolysis with Tryp would introduce a four AA N-terminal elongation and a potential one AA truncation in the C-terminal, although the Pro may also reduce efficiency (Giansanti et al., 2016). Although target AAs for both Alc and Neut are found through the peptide, the positioning of Phe residues at the termini makes γ36 a good target for partial hydrolysis. This may particularly be the case for Alc,

494 as there are substantially fewer target AAs for this protease in the sequence. In clusters 5-7, target
495 peptides have unfavourable positioning of target AAs for all three proteases, but partial hydrolysis
496 by Alc and Neut may be possible for obtaining peptides closely resembling the target.
497 Ultimately, the *in silico* analysis shows that particularly cluster 1 is an excellent target for
498 hydrolysis with Tryp. Tryp may also produce a peptide closely resembling γ36 from cluster 4. For
499 the remaining clusters, no clear evidence for release of target (or closely related peptides) was
500 found, although both Alc and Neut may produce hydrolysates containing peptides resembling the
501 targets through partial hydrolysis, where Alc may produce peptides with better emulsifying
502 properties than Neut.
503

504 *3.2.Enzymatic hydrolysis*

505 Initially, enzymatic hydrolysis was performed without heat denaturation due to the high (90%)
506 protein solubility (Table 2) in the native PPI (method A). However, a very low efficiency of
507 hydrolysis was observed. The low degree of hydrolysis was observed in the lyophilized
508 supernatant following post-hydrolysis heat inactivation of the proteases and subsequent
509 centrifugation (Fig. 3A), by comparison to the control (unhydrolyzed PPI). Only for high
510 concentrations of Flav (Fig. 3A, lane 12) and to a lesser extent Alc (Fig. 3A, lane 9), some degree
511 of hydrolysis of the patatin band (~40 kDa) could be observed. This can be ascribed to the
512 maintained inhibitory activity of wide variety of protease inhibitors inherent to potato tubers
513 (Kunitz-type ~20 kDa, PIN-type ~15 kDa, and MCPI-type ~5-10 kDa) It has been suggested that
514 in a temperature range of 55-70 °C, inhibitor activity of protease inhibitors in potato protein is
515 remarkably destroyed (Van Koningsveld et al., 2001). However, it has also been shown that even
516 after cooking of potato protein at high temperature (75-100 °C), around 10% of the chymotrypsin

517 inhibiting activity remains (Huang, Swanson, & Ryan, 1981). Application of harsh treatments,
518 such as combination of thermal coagulation and acid precipitation, may therefore destroy
519 inhibitory activity of some protease inhibitors (including aspartate-, cysteine-, and Kunitz-type
520 protease inhibitors), while other protease inhibitors may retain their inhibitory function (Waglay
521 & Karboune, 2016a). This is particularly of interest, as PTN 6.0S has been reported to exhibit
522 chymotrypsin activity (Nongonierma, Paolella, Mudgil, Maqsood, & FitzGerald, 2017). Wang and
523 Xiong (2005) investigated hydrolysis of heat-denatured potato protein by SDS-PAGE, and after
524 30 min Alc hydrolysis, the ~40 kDa band vanished as a result of patatin hydrolysis (Wang &
525 Xiong, 2005). Based on this, we hypothesized that the efficiency of enzymatic hydrolysis will be
526 enhanced if the protease inhibitors become thermally denatured and hence, method B was
527 employed. Although increased hydrolysis is desired, the degree of hydrolysis (DH) should be kept
528 low, as peptides should be above a certain length to retain emulsifying properties (García-Moreno
529 et al., 2016). The minimum length depends on peptide interfacial conformation (García-Moreno,
530 Gregersen, et al., 2020), but at least 12 AAs. This directly implies that, the DH should not exceed
531 10% and preferably be even lower (Klompong, Benjakul, Kantachote, & Shahidi, 2007; Liu, Kong,
532 Xiong, & Xia, 2010; Tamm et al., 2015). Consequently, the hydrolysis time was kept short (2 h)
533 for method B.
534

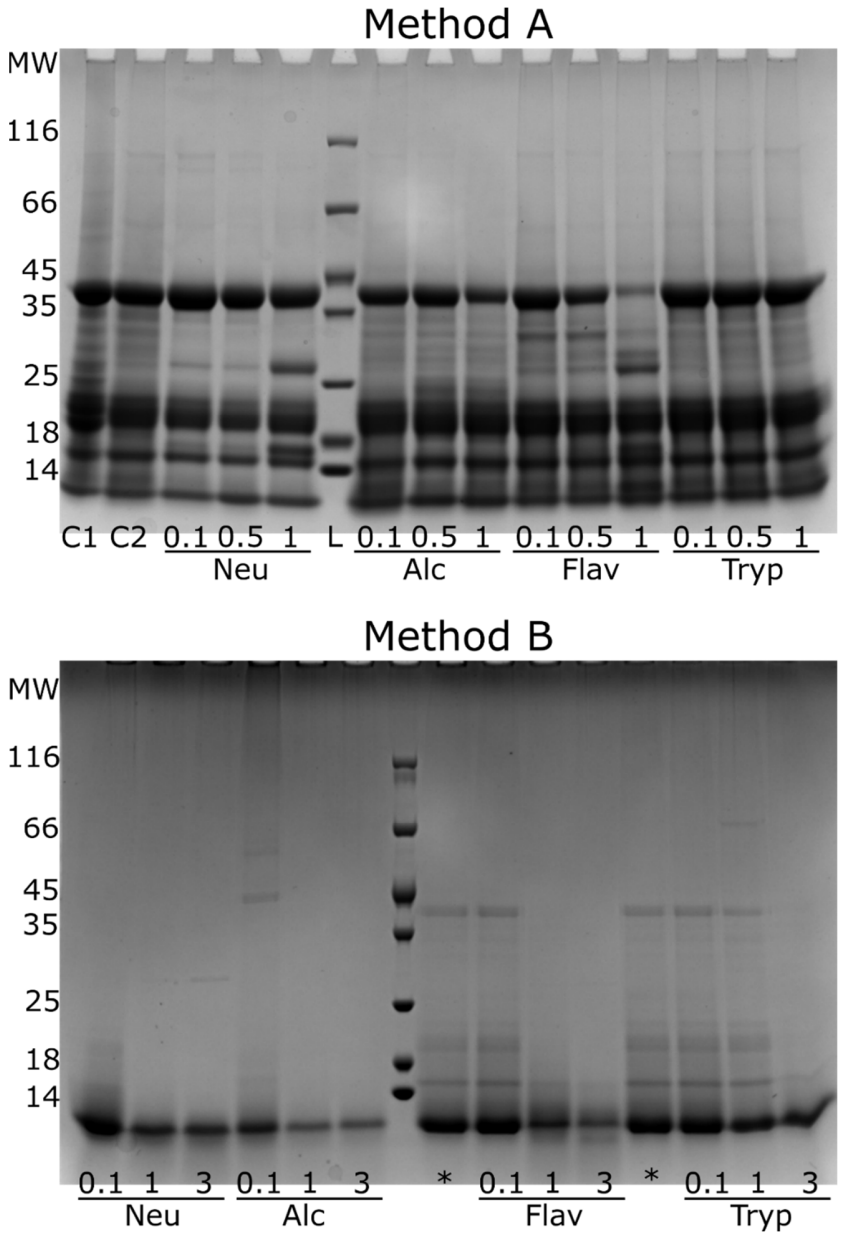

Fig. 3: SDS-PAGE of PPH (freeze-dried supernatants) following hydrolysis of native PPI (Method A) and hydrolysis of heat denatured PPI (Method B) using Neutrase (Neu), Alcalase (Alc), Flavourzyme (Flav), or Trypsin (Tryp) at different E/S ratios (Method A: 0.1%, 0.5%, and 1%. Method B: 0.1%, 1%, and 3%). C1: Native PPI. C2: Process control with native PPI. *Repetition of 0.1% hydrolysis for Flav and Tryp.

542 Enzymatic hydrolysis was conducted in a free fall pH mode, i.e., the initial pH was adjusted at 8.0,
543 but during hydrolysis gradually decreased at varying extent to a final pH of 6.8-8.0 for method B
544 (Table 2). This was done to emulate industrial scale-up, where pH control may not always be
545 possible (Kamnerdpetch et al., 2007). As expected, a relation between the extent of hydrolysis
546 (DH) and the decrease in pH was observed. All hydrolysates displayed DH within the desired
547 range (DH<8%) with the exception of 3% Neut showing significantly ($p<0.05$) higher extent of
548 hydrolysis (DH=11%). Lower DH for Flav has also been observed in other studies investigating
549 proteolysis of plant proteins (Li et al., 2015; Zhao et al., 2012). As expected, increasing E/S ratio
550 increased the efficiency of enzymatic reaction significantly ($p<0.05$), but at different extents. This
551 is supported by SDS-PAGE analysis (Fig. 3B), where a dramatic decrease of unhydrolyzed protein,
552 compared to the non-denatured PPI (Fig. 3A), can be observed particularly for higher E/S ratios.
553 This is in agreement with previous studies, where with fixed, initial substrate concentration and
554 fixed hydrolysis time, increased E/S ratio increases DH (Waglay & Karboune, 2016a).
555
556
557 **Table 2:** Hydrolysis and bulk properties of enzymatic potato protein hydrolysates (PPH)* by
558 different industrial proteases at different E/S ratios. For each PPH, the degree of hydrolysis (DH)
559 by α-amino-N determination and the associated average peptide chain length (PCL) are indicated
560 along with protein content (% by N*6.25), hydrolysis yield (%mass in freeze-dried supernatant),
561 bulk density, whiteness, and solubility (at 10 mg/mL). For comparison, bulk properties for the
562 initial substrate (potato protein isolate, PPI), sodium caseinate (SC), and a purified patatin fraction
563 are listed.

Enzyme	E/S ratio (%)	DH (%)	PCL	Protein content (%)	Yield (%)	Bulk Density (g/mL)	Whiteness	Solubility (%)	Final pH
Neutrase	0.1	2.7±0.1^{d}	36.6±1.4^{b}	80.1±0.6^{b}	15.1	0.27	68.0±0.5^{d}	91.1±1.1^{f}	7.40
	1.0	5.4±0.5^{bc}	18.1±0.9^{e}	84.3±0.3^{a}	26.1	0.27	70.7±0.5^{c}	99.2±0.6^{ab}	7.25
	3.0	10.8±1.2^{a}	9.2±0.2^{d}	83.9±1.3^{a}	39.9	0.21	68.2±0.3^{d}	99.6±0.1^{a}	6.80
Alcalase	0.1	1.2±0.0^{e}	86.8±7.2^{a}	71.6±0.3^{d}	9.7	0.11	70.2±0.8^{c}	98.7±2.5^{ab}	7.68
	1.0	5.1±0.4^{c}	19.2±1.2^{c}	74.0±0.3^{c}	13.9	0.13	71.5±0.4^{c}	98.7±0.1^{ab}	7.45
	3.0	6.2±0.5^{b}	15.8±1.1^{cd}	73.8±0.3^{c}	17.5	0.18	71.3±0.6^{c}	97.3±1.8^{bc}	7.20
Flavourzyme	0.1	1.3±0.1^{e}	71.9±17.3^{a}	69.2±0.4^{e}	8.8	0.24	66.2±0.9^{d}	93.8±2.3^{e}	8.0
	1.0	2.7±0.9^{d}	36.9±3.8^{b}	69.7±0.0^{e}	12.4	0.24	63.0±1.3^{e}	95.1±1.5^{de}	7.86
	3.0	2.9±0.6^{d}	35.4±5.1^{b}	67.4±0.1^{f}	14.4	0.43	59.3±0.5^{f}	96.6±3.5^{cd}	7.83
Trypsin	0.1	1.4±0.1^{e}	70.7±5.1^{a}	68.7±0.2^{e}	9.1	0.13	66.6±0.4^{d}	100.0±0.0^{a}	7.85
	1.0	2.9±0.2^{d}	34.9±1.6^{b}	79.7±2.1^{b}	19.5	0.10	68.4±0.3^{d}	100.0±0.0^{a}	7.53
	3.0	5.4±0.7^{bc}	18.1±1.2^{c}	83.4±0.7^{a}	29.2	0.13	70.1±0.6^{c}	96.5±0.2^{cd}	7.24
PPI*				87.0±0.2		0.29	79.8±0.2^{b}	90.4±0.7^{f}	
SC**		N/A	N/A	92.6***	N/A	0.48	86.5±0.0^{a}	99.6±0.2^{ab}	N/A
Patatin				~95****		0.25	79.4±0.3^{b}	98.9±0.1^{ab}	

* Potato protein isolate (native, before heat treatment)
** Sodium caseinate (Miprodan 30, Arla, Denamrk)
*** (Bjornshave et al., 2019)
**** Lihme Protein Solutions provided information (based elemental analysis and a N-to-protein conversion factor of 6.25) following patatin purification
Mean±SD. data are based on three replicates where possible.
Different small superscript letters in each column indicate the significant differences among means at 95 confidence level (α=0.05)

Higher proteolytic activity for Flav, compared to e.g. Alc (DH of 22% vs. 8%), has previously been reported for hydrolysis of potato pulp and attributed to the simultaneous endo- and exoproteolytic activity of Flav (Kamnerdpetch et al., 2007). Nevertheless, as the study employed substantially higher E/S ratio (7%), prolonged hydrolysis (26 h), and was performed directly on pulp, direct comparison is futile. Wang and Xiong (2005) investigated the hydrolysis of heat-denatured potato protein using Alc (1% E/S ratio) and stated that by increasing the reaction time from 0.5 h towards 1h and 6h, DH increased from 0.72 to 1.9 and 2.3%, respectively. These results are comparable to the DH obtained using Alc in our study. Although Alc is often reported to result in higher DH due to broader specificity (Demirhan, Apar, & Özbek, 2011; García Arteaga,

582 Apéstegui Guardia, Muranyi, Eisner, & Schweiggert-Weisz, 2020; Jafarpour, Gregersen, et al.,
583 2020; O'Keeffe & FitzGerald, 2014), a significantly higher ($p<0.05$) DH is observed for Neut.
584 This despite the initial pH of the hydrolysis is better aligned with optimum conditions for Alc. The
585 lower DH for Alc is, however, in line with previous studies on potato protein hydrolysis
586 (Kamnerdpetch et al., 2007; Wang & Xiong, 2005). Because a substantial amount of protease
587 inhibitory activity is retained even after heating (Van Koningsveld et al., 2001), the mode of action
588 for the applied proteases (i.e. protease families/classes) and the composition of protease inhibitors
589 in PPI becomes a limiting step. Alc is a serine protease in the subtilisin family (Aldred, Phang,
590 Conlan, Clare, & Vancso, 2008; Donlon, 2007) while Neut is a Zn-metalloprotease (Wu & Chen,
591 2011) but both exhibit endoproteolytic activity. As previously reported (García-Moreno,
592 Gregersen, et al., 2020), protease inhibitors constitute more than half of the protein in the PPI
593 (referred to as KMC-Food) used as substrate for hydrolysis. The vast majority of these are Kunitz-
594 type inhibitors, where the class of serine protease inhibitors (KTI-B) constitute a very large
595 proportion, corresponding to around 20% of the total protein (García-Moreno, Gregersen, et al.,
596 2020; Pęksa & Miedzianka, 2021). In contrast, metalloprotease inhibitors constitute a very small
597 part (>0.1%) and, importantly, are all in the form of metallocarboxypeptidase inhibitors (MCPI),
598 thereby inhibiting exoproteolytic activity (García-Moreno, Gregersen, et al., 2020; Jørgensen et
599 al., 2011; Pouvreau et al., 2001). Consequently, retained inhibitory activity against e.g. serine
600 protease like Alc may likely explain why a significantly higher DH is observed for Neut.
601 Interestingly, DH also appears to be somewhat correlated with both protein content in the PPH and
602 the yield of hydrolysis (Table 2), indicating that hydrolysis is indeed a prerequisite to resolubilise
603 the heat-denatured PPI, in line with previous studies (Miedzianka et al., 2014; Wang & Xiong,
604 2005). The significantly lower DH ($p<0.05$) observed for Flav is also reflected in significantly

605 lower ($p<0.05$) protein content and lower yields at all E/S ratios. Low yields (<20%) and a
606 substantial reduction in protein content (<80%) compared to PPI (87%) is also observed for Alc
607 and Tryp at low E/S ratios (0.1 and 1 %), thereby making such processes potentially unbeneficial
608 from an industrial and economical point of view.
609

610 *3.3.Bulk properties of PPH*

611 3.3.1. Physical properties

612 The bulk density has a substantial impact on e.g. packaging and handling attributes, as well as
613 physicochemical and sensory properties of powdery-like materials such as freeze-dried protein
614 hydrolysates (Kurozawa, Morassi, Vanzo, Park, & Hubinger, 2009; Rodríguez-Díaz, Tonon, &
615 Hubinger, 2014). In our study, PPH produced using Neut and Flav display bulk densities (0.21-
616 0.27 g/mL) within the same range as the native PPI and the enriched patatin fraction (Table 2).
617 These values are a little lower than previous reports (0.36 g/mL) for freeze-dried potato protein
618 (Claussen, Strømmen, Egelandsdal, & Strætkvern, 2007) but comparable to e.g. casein and codfish
619 hydrolysates (Jafarpour, Gomes, et al., 2020; Sarabandi, Sadeghi Mahoonak, Hamishekar,
620 Ghorbani, & Jafari, 2018).
621 Color parameters of recovered PPHs were measured using the CIE system and reported as
622 lightness (L^*), redness (a^*), and yellowness (b^*) (Table A.2) as well as the overall vector of these
623 three parameter colors, whiteness (Table 2). PPHs showed lower whiteness values compared to
624 the PPI and patatin powders ($P<0.05$). Among PPHs, the whitest (70.2-71.5) powder was obtained
625 by application of Alc, whereas Flav resulted in the lowest whiteness (59.2); particularly at highest
626 E/S ratio ($P<0.05$). Miedzianka et al. (2014) reported that application of Alc enzyme for
627 hydrolyzation of fodder potato protein significantly lightened the color of PPH powder (72.5)

628 compared to the raw sample (50.3) (Miedzianka et al., 2014). In this study, the PPI had a
629 substantially higher whiteness (79.8) whereas the whiteness of PPHs were comparable to that
630 reported by Miedzianka et al. (2014). If decreased whiteness in PPHs is related to the heat
631 treatment prior to hydrolysis, and thereby possibly a result of enzymatic browning prior to enzyme
632 denaturation (Sapers & Miller, 1992), oxidation (Tien, Vachon, Mateescu, & Lacroix, 2001), or
633 Maillard reactions (Keppler, Schwarz, & van der Goot, 2020; Liska, Cook, Wang, & Szpylka,
634 2016), was not explored further. However, the enzyme formulation may itself have direct impact
635 on the PPH color (Fig. A.1), as the Flav formulation was substantially darker than the remaining
636 formulations (Fig. A.2) and the whiteness decreased with increasing E/S ratio. Similar
637 observations have been reported for hydrolysates from round scad (Thiansilakul, Benjakul, &
638 Shahidi, 2007).
639
640 3.3.2. Emulsifying Properties
641 Turbidity measurements to quantify EAI and ESI are considered reliable indicators of emulsifying
642 properties for proteins and peptides (Pearce & Kinsella, 1978). The EAI and ESI of PPHs prepared
643 with the four proteases are shown in Table 3. In general, application of lower E/S ratios (0.1% and
644 1%) resulted in significantly lower EAI compared to controls (PPI, SC and Pat) ($P<0.05$), and only
645 Tryp 1% displayed EAI comparable to PPI and SC ($P>0.05$) but still significantly lower than native
646 Pat ($P<0.05$). In contrast, the EAI of Tryp PPHs at 3% E/S ratio was significantly higher ($P<0.05$)
647 compared to both PPI and SC and comparable to the EAI of native Pat ($P>0.05$), confirming the
648 original hypothesis based on *in silico* analysis. 3% Alc PPH also displayed EAI higher than PPI
649 and SC ($P<0.05$) but was significantly lower than both Pat and 3% Tryp PPH ($P<0.05$). At 3% E/S
650 ratio, Flav treatment resulted in a nearly equivalent ($P>0.05$) EAI compared to those from PPI and

SC, while Neut PPH displayed the lowest EAIs ($P<0.05$). That isolated, native Pat has strong emulsifying properties is in line with previous studies (Van Koningsveld et al., 2006). Using other methods to evaluate emulsifying properties than EAI (e.g. emulsion droplet size distribution and oil/water interfacial tension reduction) has, however, revealed that native Pat may not result in such strong emulsification as observed here, whereas the 3% Tryp PPH does appear to indeed have very strong emulsifying properties regardless of evaluation method (Manuscript submitted, Food Chemistry). In any case, obtaining native, isolated patatin is a costly process, and therefore not a scalable and economically viable solution.

Table 3: Emulsifying and foaming properties of enzymatic potato protein hydrolysates (PPH)* by different industrial proteases at different E/S ratios. For each PPH, the Emulsification Activity Index (EAI), Emulsification Stability Index (ESI), Foaming Capacity (FC), and Foaming Stability (FS) are indicated. For comparison, the native potato protein isolate (PPI), sodium caseinate (SC), and a purified patatin fraction are listed.

Enzyme	E/S ratio (%)	EAI (m^2/g)	ESI (min)	FC (%)	FS (%)
Neutrase	0.1	45.1 ± 0.4^{f}	22.7 ± 2.1^{fg}	100 ± 8^{g}	$28.0\pm3.4d^{c}$
	1.0	33.3 ± 2.9^{g}	67.1 ± 3.3^{a}	138 ± 10^{e}	$20.4\pm4.4d^{de}$
	3.0	52.4 ± 4.6^{ed}	25.5 ± 2.6^{ef}	98 ± 6^{g}	21.6 ± 1.5^{fd}
Alcalase	0.1	54.7 ± 4.3^{d}	21.9 ± 0.4^{fg}	288 ± 10^{d}	6.9 ± 1.2^{gh}
	1.0	52.2 ± 0.5^{ed}	26.8 ± 2.1^{e}	498 ± 10^{a}	5.4 ± 0.5^{h}
	3.0	109.5 ± 1.4^{b}	20.1 ± 1.7^{gh}	501 ± 2^{a}	7.4 ± 0.5^{gh}
Flavourzyme	0.1	48.4 ± 2.6^{ef}	31.8 ± 3.7^{cd}	380 ± 8^{c}	8.4 ± 0.9^{gh}
	1.0	30.8 ± 3.5^{g}	44.6 ± 1.6^{b}	301 ± 10^{d}	7.5 ± 0.6^{gh}
	3.0	68.0 ± 2.8^{c}	35.7 ± 2.3^{c}	400 ± 4^{b}	5.7 ± 1.2^{gh}
Trypsin	0.1	42.4 ± 4.0^{f}	31.0 ± 0.5^{d}	300 ± 8^{d}	9.3 ± 1.5^{gh}
	1.0	66.5 ± 1.9^{c}	20.8 ± 1.2^{gh}	401 ± 6^{b}	12.3 ± 0.6^{fg}
	3.0	124.2 ± 4.9^{a}	25.2 ± 2.3^{ef}	498 ± 2^{a}	15.8 ± 0.5^{ef}
PPI**		70.3 ± 4.1^{c}	18.1 ± 1.9^{hi}	120 ± 6^{f}	65 ± 0.5^{a}
SC***		64.5 ± 3.3^{c}	15.9 ± 1.2^{i}	90 ± 2^{g}	47.1 ± 3.3^{b}
Patatin		127.2 ± 1.5^{a}	11.8 ± 1.1^{j}	53 ± 2^{h}	65.2 ± 6.9^{a}

* Freeze-Dried potato protein hydrolysate (supernatant after centrifugation)
** Potato protein isolate (native, before heat treatment)

667 ***Sodium caseinate
668 Mean±SD. all data are based on three replicates
669 Different small superscript letters in each column indicate the significant differences among means at 95 confidence
670 level (α=0.05)
671

672 All PPHs in our study produced emulsions with higher ESI compared to those with PPI, SC and
673 Pat (P<0.05). The highest ESI value was determined for Neut (67.0 min) followed by Flav (44.5
674 min), both at 1% E/S. However, these PPHs also displayed the lowest values of EAI across all
675 PPHs. EAI does not follow the same trend as a function of E/S ratio (and thus DH) for the
676 investigated proteases. For instance, in case of Neut and Flav by increasing the E/S ratio from
677 0.1% to 1%, the EAI values decreased, whereas it increased significantly at 3% E/S (P<0.05). On
678 the other hand, the EAI of Tryp derived PPH, showed a constantly increasing trend with increasing
679 enzyme concentration, reaching 124 m^2/g at 3% E/S (corresponding to DH = 5.4%). EAI values
680 of Alc derived PPH showed no significant difference between 0.1 and 1% E/S ratio (P>0.05),
681 whereas it increased significantly (P<0.05) to 109 m^2/g at 3% E/S (DH = 6.2%). In line with these
682 results, Zhao and Hou (2009) reported that soy protein hydrolysates produced with Tryp (DH 1–
683 2%) exhibited a better EAI than those of hydrolyzed by Neut at the same DH (X. Zhao & Hou,
684 2009). This could be ascribed to the higher specificity of Tryp, resulting in a more well-defined
685 hydrolysate and release of peptides containing a hydrophilic C-terminus (Lys/Arg), which could
686 contribute to electrostatic stabilization of the oil droplets in the emulsion (X. Zhao & Hou, 2009).
687 Similarly, other studies revealed the superior solubility and emulsifying properties of protein
688 hydrolysates produced with Tryp (Padial-Domínguez, Espejo-Carpio, Pérez-Gálvez, Guadix, &
689 Guadix, 2020; Taherian, Britten, Sabik, & Fustier, 2011).

690 Overall, EAI and ESI did not correlate with DH nor each other directly (Fig. A.3). Diffusion
691 properties in solution highly influence the adsorption rate of emulsifiers to the oil-water interfaces
692 during homogenization (McClements & Jafari, 2018). In other words, there is a propensity for

693 smaller monomers to diffuse more quickly to an interface than a e.g. larger proteins or aggregates.
694 Despite a significantly higher DH for Neut at 3%, the EAI was less than half of the EAI for Alc
695 and Tryp derived PPHs (corresponding to DH = 6.2% and DH = 5.4%, respectively). In contrast,
696 Flav-derived PPHs displayed much lower DH (2.9%) but higher EAI than Neut PPHs. This
697 indicates that although smaller peptides diffuse rapidly and adsorb at the interface, they may indeed
698 be less efficient in stabilizing emulsions. Moreover, the results also indicate that mean peptide
699 chain length (PCL) as determined by the DH cannot be used directly as a measure of
700 emulsification, as previously shown in potato protein hydrolysates (Akbari, Mohammadzadeh
701 Milani, & Biparva, 2020). Previous studies have indicated that a minimum length (>12 AAs) is
702 required for a peptide to obtain a defined structure at the interface and thus display emulsifying
703 properties (García-Moreno, Gregersen, et al., 2020), indicating that there may be a preferred length
704 range for peptides to display emulsifying properties. Although there are no clear trends in our data,
705 it does appear that operating within a range of fairly low DH (~ 2-8%) seems to promote the
706 likelihood of obtaining a hydrolysate with improved emulsification, when evaluated by EAI and
707 ESI (Fig. A.3.A and Fig. A.3.B), but this also appear to be highly protease-dependent and not
708 universally applicable. Interestingly, there are also indications, but no strong evidence, that there
709 may be a trade-off between EAI and ESI for the hydrolysates (Fig. A.3.C). Although DH (and thus
710 PCL) is not a viable measures to estimate emulsifying activity by itself, it may be one of many
711 factors to consider; particularly in relation to avoiding excessive hydrolysis, which can
712 substantially deteriorate emulsifying activity (Klompong et al., 2007; Liu et al., 2010; Vioque,
713 Sánchez-vioque, Clemente, Pedroche, & Millán, 2000). The amphiphilicity and interfacial
714 conformation of peptides may, ultimately, outweigh peptide length as a determining factor for
715 emulsifying properties (Klompong et al., 2007).

716 Importantly, our results indicate that Tryp is indeed capable of producing a PPH with significantly
717 improved emulsifying properties compared to both other industrially relevant proteases and the
718 substrate itself. In fact, only the application of Tryp was able to improve both emulsification
719 activity and stability significantly ($P<0.05$), compared to untreated PPI. These observations are in
720 line with the predicted and expected outcome based on prior knowledge and *in silico* analysis,
721 which indicates the potential release of known emulsifier peptides from potato protein when using
722 Tryp. This highlights that a data-driven, targeted approach for enzymatic hydrolysis is a promising
723 and viable approach for optimizing the functional parameters of industrial side streams such as
724 potato protein. And that this may be obtained in a predictable manner, alleviating the need for
725 conventional trial-and-error methodology.

726

727 3.3.3. Foaming properties

728 A common way to evaluate the foaming properties of products such as hydrolysates, is by
729 determinination of their foaming capacity (FC) and stability (FS), describing different molecular
730 properties related to stabilization of the air/water interface (Petruccelli & Anon, 1995; Ralet &
731 Guéguen, 2000). In our study, apart from Neut-derived PPHs at 0.1% and 3% E/S ratio, all PPHs
732 showed significantly higher ($P<0.05$) FC compared to control samples. In contrast to the
733 emulsifying properties, the highest FC of the control samples was determined for PPI, followed by
734 SC, and patatin, respectively ($P<0.05$). The PPHs from Alc and Tryp showed remarkably high
735 (~500%) but comparable ($P>0.05$) FC at high E/S ratio (3%) (Table 3). These results imply that
736 there is no direct relationship between foaming capacity and DH (Fig. A.4.A). Conformational
737 properties of released peptides relies highly on the specificity of the applied protease. For instance,

738 the lower FC as well as EAI of Neut-derived PPH may be attributed to a sequence-specific and
739 lower surface activity of released peptides rather than their average length; similarly as was
740 observed for emulsifying properties. That being said, the decrease in FC with a decrease in E/S
741 ratio from 1% to 3% may also be the result of extensive hydrolysis, ultimately releasing too short
742 peptides with a decreased propensity to form defined structures at the interface. This is in
743 agreement with previous studies on Alc hydrolysis of a potato protein isolate, where extending
744 hydrolysis time, increased DH up to 17%, which resulted in a decrease in FC (Akbari et al., 2020).
745 Such high DH was not observed for Alc (or other) PPHs in this study, which could explain why
746 the effect was only seen for Neut-derived PPHs as all other PPH had a DH in the range from 1.2%
747 - 6.2% (Table 2).

748 Control samples showed higher ($P<0.05$) stability compared to PPHs (Table 3), as the highest FS
749 (~65%) was determined for the native PPI and the patatin fraction ($P>0.05$), followed by SC at
750 ~47% ($P<0.05$). For PPHs, the highest FS was determined for Neut followed by Tryp PPHs, while
751 both Alc and Flav PPHs presented the lowest FS (<10%) among all ($P<0.05$). Increasing the Neut
752 E/S ratio from 0.1% to 3% caused a significant decrease ($P<0.05$) in stability of formed foams
753 from 28% to about 22% ($P<0.05$), whereas the inverse effect was observed for Tryp, where
754 increasing E/S from 0.1% to 3% significantly increased FS from ~9% to ~16% ($P<0.05$). Between
755 Alc and Flav PPHs, there was no significant difference ($P>0.05$) in determined FS. Interestingly,
756 only hydrolysis by Tryp improved both FC and FS (as well as EAI) with increasing DH. In earlier
757 studies, the FC and FS of a potato protein concentrate (8% and 5.3%, respectively) increased to
758 162% and 51% after hydrolysis by Alc for 2h (Miedzianka et al., 2014). Although these values are
759 not in full agreement with our data, the study also highlights the positive effect of proteolysis for
760 increasing the surface activity, as well as solubility, compared to the protein substrate. In our study,

761 Alc and Tryp hydrolysis at 3% E/S ratio resulted in both comparable FC (~500%) and DH (~6%),
762 but remarkably different FS. Foams produced with 3% Tryp PPH had double the stability of 3%
763 Alc-derived PPH (Table 3). No apparent relation between DH and FS was observed (Fig. A.4.B)

764 Similarly to the relation between EAI and ESI, there appears to be a general trade-off between FC
765 and FS (Fig. A.4.C), although e.g. Tryp PPHs shows the opposite trend. While control samples
766 (PPI, SC, and Pat) produce the most stable foams, they produce the least stable emulsions.
767 Hydrolysis of PPI (as well as native Pat) significantly increases the capacity to foam ($P<0.05$), but
768 also significantly decreases the foam stability ($P<0.05$), in line with the general observations of a
769 negative relation between FC and FS for PPHs in this study. Although no clear correlation is
770 observed, there does appear to be some relation between high emulsifying and foaming capacities
771 (Fig. A.5.A), indicating that to some extent, similar molecular properties are involved in both
772 interfacial properties, in line with previous studies (Wouters, Rombouts, Fierens, Brijs, & Delcour,
773 2016). The stability of the interfaces, however, appear to be governed by different forces and
774 properties, and no apparent relation (Fig. A.5.B).

775
776

777 *3.4.Peptide identification and mean peptide properties*

778 Across the 12 PPHs investigated with LC-MS/MS, unspecific analysis in MaxQuant resulted in
779 identification of 46,316 unique peptides following removal of reverse and contaminant peptides.
780 Although a higher FDR (5%) was applied for MaxQuant analysis, this level was previously shown
781 to be suitable for non-specific digests due to the significantly increased combinatorial search space
782 (Gregersen et al., 2022). In general, a lower number of peptides were identified in PPHs produced
783 using Neut, although more than 10,000 peptides were identified in all PPHs (Table 4). This is a

784 tremendous increase in depth of analysis compared to previous reports of LC-MS/MS analysis on
785 hydrolysates, where the number of identified peptides is often reported in the tens to low thousands
786 range (Caron et al., 2016; Cui, Sun, Cheng, & Guo, 2022; Hinnenkamp & Ismail, 2021; Y. P.
787 Huang, Dias, Leite Nobrega de Moura Bell, & Barile, 2022; Jafarpour, Gregersen, et al., 2020; Jin,
788 Yan, Yu, & Qi, 2015; M. Li, Zheng, Lin, Zhu, & Zhang, 2020).
789
790
791
792 **Table 4**: Summary statistics for identified peptides (Peptide IDs) and peptide weighted average
793 length (PCL_{avg}) by unspecific analysis of potato protein hydrolysate (PPH) LC-MS/MS data in
794 MaxQuant. The total peptide MS1 intensity (Σ Int) for each PPH is listed along with the associated
795 normalization factor (NF) used for relative, peptide-level comparison.

Enzyme	Alcalase			Flavourzyme			Neutrase			Trypsin		
E/S ratio	0.1%	1%	3%	0.1%	1%	3%	0.1%	1%	3%	0.1%	1%	3%
Peptide IDs	13140	14106	13125	14622	12936	13094	12210	11944	10829	14948	12756	12475
Total		19513			21976			17356			23509	
PCL_{avg}	15.9	15.3	14.9	15.8	14.8	14.5	14.2	13.2	12.7	15.9	15.8	15.0
Σ Int [$1E^{12}$]	8.7	12.2	13.2	6.9	5.5	8.1	13.6	12.0	9.3	5.7	10.6	13.7
NF	0.638	0.889	0.966	0.502	0.399	0.589	0.996	0.877	0.683	0.420	0.773	1

796
797 As expected, changing hydrolysis conditions by increasing E/S ratio, and thereby increasing DH,
798 had a substantial effect on the number and nature of identified peptides for all four investigated
799 proteases. This is illustrated both by the number of identified peptides (Table 4) as well as shared
800 peptides between PPHs obtained using the same protease (Fig. A.6). Interestingly, the effect of
801 protease and E/S ratio on DH, determined through α-amino nitrogen quantification (Table 2), is

not to the same extent reflected in the peptide level data, using intensity-weighted peptide abundance estimation, PCL_{avg} (Table 4). This is in contrast to previous studies, where a much stronger correlation between the two methods was observed (Jafarpour, Gregersen, et al., 2020). However, there are notable differences between the two studies. In Jafarpour et al. (2020), hydrolysis was performed on a raw side stream from the cod industry, where this study deals with a much purer protein isolate. This is clearly illustrated by the lack of distinct protein bands in SDS-PAGE analysis in the cod hydrolysates, where we here observed strong bands from intact protein and larger protein fragments by SDS-PAGE following hydrolysis (Fig. 3), indicating that a substantial amount of protein remains in forms undetectable using a bottom-up proteomics approach. According to Linderstrøm-Lang theory, proteases may have higher affinity for intermediate fragments/peptides than intact proteins (Adler-Nissen, 1986; Linderstrøm-Lang, 1953). It was previously shown in e.g. milk (Deng, van der Veer, Sforza, Gruppen, & Wierenga, 2018; Hinnenkamp & Ismail, 2021) and rice (Nisov, Ercili-Cura, & Nordlund, 2020) as well as potato (Akbari et al., 2020; Pęksa & Miedzianka, 2014) proteins, that this is indeed the case in a highly protein- and protease-specific manner. This also suggests that the observation of intense bands for residual intact protein by SDS-PAGE (Fig. 3), should likely not be interpreted as lack of hydrolytic activity, but rather increased protease affinity for intermediate fragments/peptides. Similarly, hydrolysis to the single AA and dipeptide level will contribute significantly to the total DH of a sample, while these remain undetected in the MS experimental design. Nevertheless, a decrease in PCL_{avg} is observed with increasing E/S ratio for each protease, and substantially lower PCL_{avg} values are obtained for Neut corresponding to the higher DH in these PPHs. This shows that even in spite of the challenges imposed by intact protein and other undetected species, MS

824 data and PCL_{avg} can provide an indication for the progression of hydrolysis in addition to peptide-
825 and protein-level insight.
826
827 *3.5.Identification of known peptide emulsifiers from potato proteins*
828 Based on emulsifying properties of the PPHs, a deeper peptide-level analysis of peptides
829 associated with the seven sequence clusters associated with known and highly potent emulsifiers
830 (Section 3.1) was performed. As the major constituents of the potato proteome (i.e. patatin and
831 protease inhibitors) all represent a large number of protein isoforms, mapping peptides to the
832 isoforms is a challenging task. This is particularly the case as single AA substitutions and minor
833 truncations/elongations may not have a detrimental effect of the peptide functionality (Enser et al.,
834 1990; García-Moreno, Gregersen, et al., 2020; García-Moreno, Jacobsen, et al., 2020; Ricardo et
835 al., 2021). To accommodate this, we established a workflow, where identified peptides were
836 mapped onto representative target cluster sequences (Fig. 2) by defining lead protein sequence
837 clusters (Table 1). The workflow allows for determining the degree of overlap between identified
838 peptides and the representative cluster sequence while allowing for substitutions, truncations, and
839 elongations. By using the peptide MS1 intensity as an estimate of abundance, it is thus possible to
840 determine how much of the peptide MS1 intensity for the whole PPH is constituted by peptides
841 adhering to both the length requirement and a minimum sequence overlap with a given target
842 cluster. As the total MS1 intensity varies substantially between PPHs (Table 4), unhydrolyzed
843 proteins content varied between PPHs, and the same total amount was loaded on-column (1µg),
844 total MS1 intensities were normalized relative to the PPH with the highest MS1 intensity (Tryp
845 3%). After applying the normalization factors (Table 4), the normalized, relative MS1 intensity
846 constituted by peptides with >50%, >75%, and >95% overlap with each of the seven target clusters,

was determined for each PPH using both a 12 AA (Fig. 4, left) and 15 AA (Fig. 4, right) minimum length requirement. From here, we see that peptides mapping to target peptide clusters 1 and 3 account for the largest contributions of mapped peptides regardless of required sequence overlap and length requirement. We also see that peptides mapping to clusters 2, 5, and 6 have practically no contribution to the sum, while the contribution from cluster 4 and 7 peptides is low. Moreover, we observe a shift in which PPHs has the highest relative contribution to overlapping peptides, based on the requirement of degree of overlap.

		12AA minimum length											
		Alcalase			Flavourzyme			Neutrase			Trypsin		
		0.1%	1%	3%	0.1%	1%	3%	0.1%	1%	3%	0.1%	1%	3%
>50%	C1	2.6%	5.9%	6.7%	2.1%	4.9%	7.0%	1.4%	2.3%	1.4%	1.8%	0.7%	0.9%
	C2	0.0%	0.0%	0.0%	0.0%	0.0%	0.0%	0.0%	0.2%	0.3%	0.0%	0.1%	0.1%
	C3	6.8%	11.3%	8.9%	4.1%	3.5%	4.3%	5.0%	4.5%	3.5%	3.9%	4.9%	3.8%
	C4	2.0%	2.8%	3.1%	1.9%	1.8%	2.4%	2.5%	2.0%	1.0%	1.4%	1.9%	3.2%
	C5	0.0%	0.0%	0.0%	0.0%	0.0%	0.0%	0.0%	0.1%	0.1%	0.0%	0.0%	0.0%
	C6	0.9%	0.8%	1.1%	2.5%	0.6%	1.0%	1.1%	0.1%	0.1%	1.9%	4.1%	3.0%
	C7	1.1%	2.3%	2.4%	0.7%	0.8%	1.2%	2.8%	1.6%	0.8%	0.6%	0.1%	0.2%
	Sum	13.4%	23.1%	22.4%	11.3%	11.7%	15.9%	12.8%	10.8%	7.1%	9.6%	11.9%	11.2%
>75%	C1	0.4%	0.7%	0.4%	0.9%	3.2%	5.8%	1.2%	2.1%	1.2%	0.7%	0.3%	0.7%
	C2	0.0%	0.0%	0.0%	0.0%	0.0%	0.0%	0.0%	0.1%	0.3%	0.0%	0.0%	0.0%
	C3	2.1%	3.1%	1.8%	3.6%	3.0%	3.7%	5.0%	4.4%	3.4%	3.5%	4.5%	3.6%
	C4	0.7%	0.8%	1.2%	0.9%	1.0%	1.2%	2.0%	1.7%	0.6%	0.8%	0.8%	1.2%
	C5	0.0%	0.0%	0.0%	0.0%	0.0%	0.0%	0.0%	0.0%	0.0%	0.0%	0.0%	0.0%
	C6	0.0%	0.0%	0.0%	0.0%	0.0%	0.0%	0.0%	0.0%	0.0%	0.0%	0.0%	0.0%
	C7	0.9%	1.8%	2.0%	0.6%	0.8%	1.1%	2.7%	1.5%	0.7%	0.6%	0.1%	0.1%
	Sum	4.0%	6.3%	5.4%	6.0%	8.0%	11.9%	11.0%	9.9%	6.3%	5.5%	5.8%	5.7%
>95%	C1	0.1%	0.2%	0.2%	0.2%	1.2%	1.5%	1.0%	1.5%	0.9%	0.2%	0.2%	0.7%
	C2	0.0%	0.0%	0.0%	0.0%	0.0%	0.0%	0.0%	0.0%	0.0%	0.0%	0.0%	0.0%
	C3	0.9%	0.6%	0.2%	2.9%	2.7%	3.2%	4.9%	4.4%	3.4%	3.0%	3.9%	3.5%
	C4	0.1%	0.2%	0.3%	0.3%	0.6%	0.5%	0.3%	0.7%	0.3%	0.3%	0.0%	0.0%
	C5	0.0%	0.0%	0.0%	0.0%	0.0%	0.0%	0.0%	0.0%	0.0%	0.0%	0.0%	0.0%
	C6	0.0%	0.0%	0.0%	0.0%	0.0%	0.0%	0.0%	0.0%	0.0%	0.0%	0.0%	0.0%
	C7	0.1%	0.2%	0.3%	0.4%	0.7%	0.9%	1.6%	1.1%	0.5%	0.3%	0.0%	0.0%
	Sum	1.1%	1.2%	1.0%	3.7%	5.1%	6.0%	7.8%	7.6%	5.1%	3.7%	4.2%	4.3%

	15AA minimum length											
	Alcalase			Flavourzyme			Neutrase			Trypsin		
	0.1%	1%	3%	0.1%	1%	3%	0.1%	1%	3%	0.1%	1%	3%
C1	2.3%	5.5%	6.2%	1.5%	2.8%	4.4%	1.3%	2.0%	1.1%	1.2%	0.6%	0.8%
C2	0.0%	0.0%	0.0%	0.0%	0.0%	0.0%	0.0%	0.1%	0.2%	0.0%	0.1%	0.1%
C3	5.6%	9.1%	7.2%	3.0%	1.5%	1.7%	4.6%	3.5%	2.4%	2.8%	3.5%	1.7%
C4	1.5%	2.4%	2.7%	1.0%	0.7%	1.0%	1.3%	1.2%	0.7%	0.8%	1.7%	2.9%
C5	0.0%	0.0%	0.0%	0.0%	0.0%	0.0%	0.0%	0.0%	0.0%	0.0%	0.0%	0.0%
C6	0.2%	0.1%	0.1%	0.8%	0.0%	0.1%	0.0%	0.0%	0.0%	0.6%	1.3%	0.7%
C7	1.0%	2.1%	2.3%	0.1%	0.1%	0.1%	1.1%	0.5%	0.2%	0.1%	0.1%	0.2%
Sum	10.7%	19.2%	18.5%	6.5%	5.2%	7.3%	8.3%	7.3%	4.5%	5.6%	7.2%	6.4%
C1	0.4%	0.5%	0.3%	0.7%	2.2%	3.9%	1.2%	1.8%	0.9%	0.5%	0.3%	0.7%
C2	0.0%	0.0%	0.0%	0.0%	0.0%	0.0%	0.0%	0.1%	0.2%	0.0%	0.0%	0.0%
C3	0.9%	0.9%	0.1%	2.5%	1.1%	1.2%	4.5%	3.4%	2.2%	2.5%	3.1%	1.6%
C4	0.3%	0.5%	0.8%	0.4%	0.3%	0.5%	0.9%	0.9%	0.3%	0.3%	0.6%	1.0%
C5	0.0%	0.0%	0.0%	0.0%	0.0%	0.0%	0.0%	0.0%	0.0%	0.0%	0.0%	0.0%
C6	0.0%	0.0%	0.0%	0.0%	0.0%	0.0%	0.0%	0.0%	0.0%	0.0%	0.0%	0.0%
C7	0.8%	1.6%	1.9%	0.1%	0.1%	0.1%	1.1%	0.4%	0.2%	0.1%	0.1%	0.1%
Sum	2.3%	3.5%	3.2%	3.7%	3.6%	5.7%	7.7%	6.6%	3.8%	3.4%	4.1%	3.4%
C1	0.0%	0.2%	0.1%	0.1%	0.4%	0.2%	1.0%	1.5%	0.9%	0.1%	0.2%	0.7%
C2	0.0%	0.0%	0.0%	0.0%	0.0%	0.0%	0.0%	0.0%	0.0%	0.0%	0.0%	0.0%
C3	0.3%	0.0%	0.0%	1.8%	0.7%	0.6%	4.4%	3.4%	2.2%	2.0%	2.4%	1.5%
C4	0.0%	0.1%	0.2%	0.1%	0.1%	0.0%	0.0%	0.0%	0.0%	0.0%	0.0%	0.0%
C5	0.0%	0.0%	0.0%	0.0%	0.0%	0.0%	0.0%	0.0%	0.0%	0.0%	0.0%	0.0%
C6	0.0%	0.0%	0.0%	0.0%	0.0%	0.0%	0.0%	0.0%	0.0%	0.0%	0.0%	0.0%
C7	0.0%	0.1%	0.2%	0.0%	0.0%	0.0%	0.1%	0.0%	0.0%	0.0%	0.0%	0.0%
Sum	0.4%	0.4%	0.5%	2.0%	1.2%	0.9%	5.5%	4.9%	3.1%	2.1%	2.7%	2.2%

Fig. 4: Heat maps (blue (low) to red (high)) of quantitative (by MS1 I_{rel}) sequence overlap between identified peptides and the target cluster sequence for all seven target cluster (C1-C7). Overlaps are given with increasing minimum overlap (50%, 75%, 95% (top to bottom)) and increasing minimum peptide length (12 AAs (left) and 15 AAs (right)) requirements. Sums across all clusters for each condition are color coded separately from the individual clusters to illustrate overall adherence of PPH peptides to all target clusters.

Interestingly, target cluster overlap (Fig. 4) overall shows low agreement with observed emulsifying properties of the PPHs (Table 3). While a low degree of overlap (>50%) shows that Alc PPHs (particularly at 1% and 3% E/S which also show high EAI) has the highest proportion of overlapping peptides, increasing requirement of sequence overlap shift the highest proportion of overlapping peptides towards Flav and Neut PPHs (which show lowest EAI), while Alc PPHs here show the lowest proportion. In all cases, Tryp PPHs (showing highest EAI), show an intermediate proportion of overlapping peptides in comparison and a low content of cluster 1 peptides, which were the primary target by Tryp hydrolysis. This observation led us to investigate if certain regions of a target cluster may be more important. By extracting the sequences for high intensity peptides in each PPH with >50% overlap in cluster 1 and 3 (Table A.3), it is possible to see that Neut PPHs contain abundant peptides overlapping with cluster 1, but that all are located in the C-terminal region of the cluster (Fig. 5, left). In contrast, high intensity Alc peptides are found in the N-terminal region of the cluster. While high intensity Flav peptides are located in both cluster termini, Tryp PPH peptides, particularly at 3% E/S, span more of the cluster (Fig.5, left). This indicates that the N-terminal region of the cluster may be of higher importance, and, more importantly, that peptides also should cover at least a certain part of the cluster to attain the interfacial activity. This is in agreement with previous studies (Yesiltas et al., 2021), where cluster 1 peptides (e.g. γ105) are highly truncated in the C-terminal region of the target cluster sequence. As such the region covered by γ105 (GIIPGTILEFLEGQLQK) may be regarded as the core region of cluster 1 and could represent a “critical region” for emulsifying activity, as this region produces a highly amphiphilic α-helix at the interface. With the exception of γ1 (which is cleaved by trypsin after Lys in position 3 resulting in γ75), all cluster 1 peptides (full length and/or full length isoforms) were identified in the 3% Tryp PPH (Table A.4). Some were also identified in the 1%

882 Tryp PPH, while very minute amounts (<0.002% I_{rel}) were found in 3% Flav PPH, both verifying
883 that target peptides were indeed released in a targeted manner and that observed differences in
884 emulsifying activity may be ascribed to substantial presence of these highly functional peptides.
885 Nevertheless, this type of analysis only describes a subpopulation of the entire, complex PPH, and
886 does not account for all other peptides and their potential (positive or negative) contribution to the
887 bulk functionality of the PPHs. Our results also indicate that a quite substantial amount of Tryp
888 was needed to efficiently release the peptides, which may be ascribed to residual inhibitory activity
889 in the PPH despite heat treatment.
890

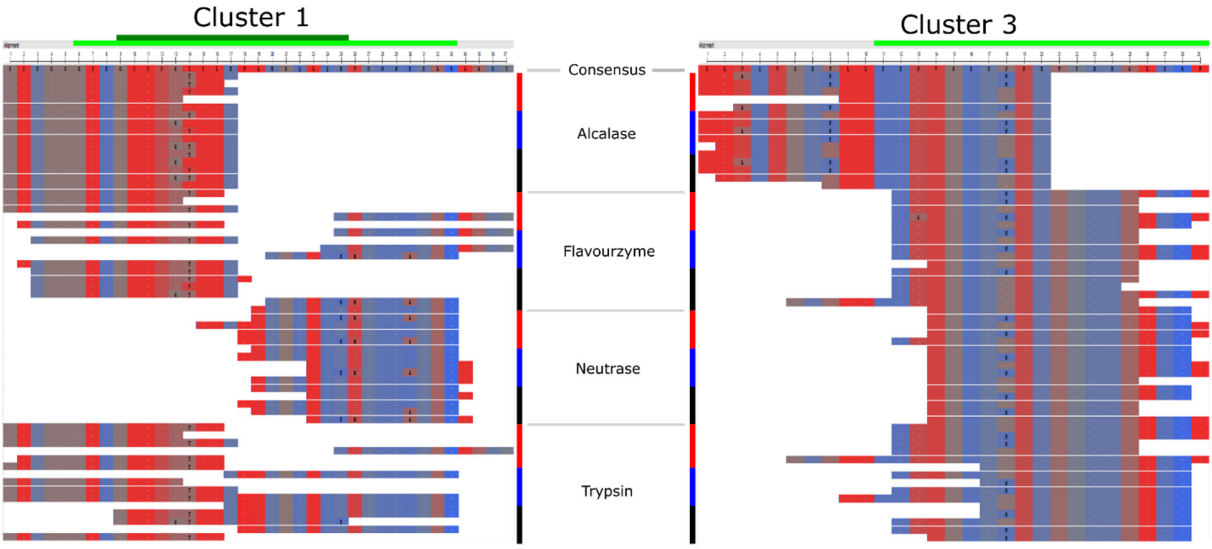

891

892 **Fig 5:** Alignment of top-5 high intensity peptides in Alc, Flav, Neut, and Tryp (top to bottom)
893 PPHs for 0.1% (red), 1% (blue), and 3% (black) E/S ratio. Only peptides with at least 50% overlap
894 with the target cluster consensus sequence for Cluster 1 (left) and Cluster 3 (right) are shown. For
895 each condition (protease and E/S ratio), the top-5 peptides are depicted with descending relative
896 MS1 intensity (top to bottom). Amino acids are color coded from red (hydrophobic) to blue
897 (hydrophilic) according to the NCBI MSA Viewer hydropathy color scale. The consensus

sequence for each cluster is shown by a light green bar (top), while the suggested "core region" for cluster 1 peptides is shown in dark green. The consensus sequence was extended in both termini to allow for full mapping and visualization of all top-5 overlapping peptides. Single amino acid substitutions (relative to the consensus sequence) are assigned by the substituent single letter code on the individual peptide level.

Cluster 3 peptides constitute the majority of all overlapping cluster peptides. With increasing requirements for both length and degree of overlap, the highest proportion shifts from Alc PPHs to Flav and particularly Neut and Tryp PPHs (Fig. 4). Cluster 3 represents two patatin-derived peptide emulsifiers, α10 and α12, which were previously shown to indeed adopt a helical conformation at the oil/water interface (García-Moreno et al., 2021). High intensity Flav, Neut, and Tryp peptides all appear to cover a significant amount of the target cluster sequence (Fig. 5, right), which intuitively should make all these PPHs good emulsifiers. Nevertheless, if assuming a helical conformation with 3.6 AA per turn, the distribution of AAs in these peptides do not appear favourable for producing an amphiphilic helix. Particularly high intensity Neut peptides are slightly truncated in the N-terminal region of the cluster, making the characteristic pattern of AA distribution in an amphiphilic helix (Eisenberg, Weiss, & Terwilliger, 1982; García-Moreno, Gregersen, et al., 2020; Yesiltas et al., 2021) absent, to a large degree. In contrast, Alc peptides extend N-terminally of the consensus sequence in cluster 3. This means that peptides include a region, which have a highly favourable AA distribution for adopting a highly amphiphilic helical conformation at the interface, and also forms an amphipathic helix in native patatin (Fig. A.7). Furthermore, the most abundant cluster 3 peptides in Alc PPHs (Fig. 5, right) are variants of the same peptide (LLAQVGENLLKKPVSKDNPE), containing either single AA substitutions or

minor (1-2 AA) N-terminal truncations, which are likely to not have substantial effect on the interfacial properties. Furthermore, most of these peptides have a highly hydrophobic N-terminus, similarly to the cluster 1 core sequence, which may serve as a hydrophobic anchor to facilitate stronger adsorption to the oil/water interface and high emulsion capacity. As Tryp and, to a lesser degree, Flav peptides also extend into this region compared to Neut peptides, this may be a key part of why Alc PPHs also show good emulsifying properties and why Flav PPHs perform better than Neut PPHs.

Although the contribution from cluster 4 peptides is smaller than cluster 1 and 3 peptides, it is noteworthy that a peptide (LADYFDVIGGTSTGGLLTAMITTPNENNRPFAAAK), corresponding to a slightly elongated version of γ36 (FDVIGGTSTGGLLTAMITTPNENNRP), was identified in all Tryp PPHs, exactly as predicted (Section 3.1). With increasing E/S ratio, the estimated abundance of this peptide also increased from 0.08% (I_{rel}) in 0.1% Tryp to 0.64% (I_{rel}) in 3% Tryp (Table A.4). This in spite of the total MS1 intensity more than doubled in 3% Tryp, indicating that increasing the DH towards completion for tryptic hydrolysis, substantially increases the release of the target peptide. This also correlates well the high emulsifying and foaming properties observed for 3% Tryp PPH. The peptides was surprisingly also identified in all Alc and Flav PPHs, but at a substantially lower abundance ($I_{rel} < 0.05\%$). In Alc PPHs, several peptides of sufficient length for helical surface activity (>15 AAs) and covering the most of γ36, were identified at noteworthy I_{rel} (Table A.4). This is particularly the case in 3% Alc, where five peptides (16-34 AAs) were identified with $I_{rel} > 0.1\%$ (0.14-0.35%). In contrast, the most abundant cluster 4 peptides in e.g. 3% Neut (0.44-0.63%) were substantially shorter (12-16 AAs) and only covering the N-terminal part of the γ36 target sequence. This adds to the peptide-level evidence,

943 substantiating why Tryp, but also Alc, PPHs have significantly higher emulsifying activity than
944 Neut PPHs.
945 Peptide-centric analysis further indicates that mapping identified peptides onto a target cluster
946 consensus sequence alone is not enough to describe high surface activity, but that a higher degree
947 of peptide-level detail is needed. It also calls for further investigations to determine which parts of
948 the target cluster sequences constitute the utmost important (core) region for functionality, thereby
949 facilitating efficient peptide mapping that correlates with observed functionality. This may be
950 addressed computationally through development of more sophisticated predictors, able to identify
951 not only core regions but also other structural features of importance for emulsifying activity in
952 addition to amphiphilicity, such as hydrophobic anchors. Moreover, estimating the
953 abundance/concentration of a specific peptide merely by the MS1 intensity is a very rough
954 estimate, as intrinsic and sequence specific properties makes peptides behave and ionize differently
955 in MS (Jafarpour, Gregersen, et al., 2020; Jarnuczak et al., 2016; Sinitcyn, Rudolph, & Cox, 2018).
956 This highlights the need for fundamentally new computational approaches for absolute peptide
957 quantification in highly complex mixtures such as hydrolysates, which is currently under
958 investigation in our lab. This would allow a more accurate evaluation of peptide release and the
959 direct, quantitative comparison between peptides rather than using raw MS1 estimation, which
960 may be biased on the single peptide-level.
961 Interestingly, high intensity cluster 1 and 3 Alc peptides (Fig. 5 and Table A.3) indicate that Alc
962 has strong preference to cleave after particularly Glu and Leu in both the N- and C-terminal.
963 Similar trends were observed for high intensity cluster 4 Alc peptides (Table A.4). While Leu
964 specificity was described by the manufacturer, Glu specificity was not. Nevertheless, this is in line
965 with previous reports on Alc specificity (Doucet et al., 2003; Lu et al., 2021). These inconsistencies

966 highlight a crucial aspect for successful application of the presented methodology. In addition to
967 the need for core region mapping and accurate peptide abundance estimation, a high degree of
968 insight on protease specificity is pivotal for making accurate *in silico* analysis and prediction of
969 peptide release. This task is significantly easier to perform for highly specific proteases (e.g.
970 trypsin), also highlighting the need for further development of high specificity industrial proteases,
971 available in bulk amounts for cost-effective process design.
972

973 *3.6.Protease and E/S ratio governs differential protein family selectivity in heat denatured PPI*

974 Using our previously published method for relative protein abundance estimation using length-
975 normalized, relative MS1 intensity (Gregersen et al., 2021, 2022), it is possible to obtain insight
976 on which proteins are abundantly represented in a hydrolysate and thereby also on protein-level
977 enrichment and selectivity. By summing intensities for all peptides originating from the proteins,
978 the potential peptide-level bias is alleviated to a large degree. This is the prerequire assumption
979 used in the iBAQ approach for relative protein quantification (Schwanhüusser et al., 2011). A
980 similar approach was recently developed for non-conventional bottom-up proteomics data, where
981 a specific protease has not been applied in the sample preparation and downstream data analysis
982 (Gregersen et al., 2021, 2022), thereby making the approach suitable for the MS data obtained in
983 this study. Based on relative abundance by I_L^{rel}, protein-level abundances were pooled into major
984 protein families/classes found in potato (Fig. 6, Table A.5). Compared to a previous study on the
985 same PPI (García-Moreno, Gregersen, et al., 2020), patatin is enriched in Alc PPHs while
986 somewhat depleted in Tryp PPHs. In fact, patatin represents more than double of the relative
987 protein content in Alc PPHs (40-45%) compared to Tryp PPHs (18-19%) at 1% and 3% E/S ratio.
988 The direct opposite is observed for Kunitz peptides, where Tryp PPHs at 1% and 3% E/S ratio

contain twice the relative amount (46-54%) compared to Alc PPHs (23-25%). As both Alc and Tryp are serine endoproteases (Peyronel & Cantera, 1995), this is likely a direct result of different specificities, and that Alc is capable of hydrolysing patatin to a much higher degree prior to inhibition by Kunitz serine protease inhibitor (KTI-B class) activity remaining despite heat treatment. This observation also correlates well with why the relative protein class distribution for Neut PPHs to a much higher extent reflects earlier MS-based proteomics studies of the PPI (García-Moreno, Gregersen, et al., 2020), as Neut is a Zinc-protease and limited inhibitory activity is expected in the PPI, as discussed in Section 3.2.

For all subclasses of Kunitz-type inhibitors and the class proteinase inhibitors (PIN), substantial differences are observed across PPHs and in comparison to our previous study on native PPI. This is of particular interest for the patatins, KTI-A, and KTI-B classes, as these represent all the target peptides (Table 1). As ten of the 15 target peptides originate from patatin isoforms, enrichment of patatin-derived peptides may be a direct reason for the strong emulsifying properties of the Alc PPH (Fig. 6), even though Tryp PPH was both predicted to have better emulsifying properties as well as shown to contain peptides with better target peptide overlap in the high abundance target clusters 1 and 3. This also illustrates that there is room for improving the interfacial properties of Tryp PPHs even more, by improving hydrolysis conditions and obtaining a higher relative amount of patatin-derived peptides in the PPH. This may potentially be accomplished by combing enzymatic hydrolysis with other methods such as e.g. ultrasound and microwave treatment, previously shown to improve digestibility of potato protein (Cheng et al., 2017; Falade, Mu, & Zhang, 2021; Mao, Wu, Zhang, Ma, & Cheng, 2020).

	Alcalase			Flavourzyme			Neutrase			Trypsin		
Class	0.1%	1%	3%	0.1%	1%	3%	0.1%	1%	3%	0.1%	1%	3%
Patatin	43.4%	45.1%	40.1%	31.4%	41.3%	36.4%	30.8%	27.6%	27.2%	31.6%	18.6%	18.4%
Kunitz_sum	25.8%	22.9%	24.6%	39.1%	25.2%	28.9%	41.1%	45.6%	48.0%	39.9%	50.3%	46.2%
KTI-A	0.2%	0.2%	0.3%	0.7%	0.3%	0.6%	1.2%	1.0%	0.7%	0.5%	0.9%	0.7%
KTI-B	14.0%	11.4%	11.3%	24.3%	14.8%	16.8%	15.9%	16.5%	16.7%	25.5%	21.6%	16.9%
KTI-C	2.3%	3.6%	4.9%	5.0%	3.0%	4.1%	11.8%	12.4%	12.4%	4.5%	15.0%	13.6%
KTI-D	2.3%	1.4%	1.5%	4.0%	2.7%	1.6%	1.7%	1.5%	1.5%	3.9%	2.0%	2.1%
Kunitz_unclassified	6.9%	6.4%	6.7%	5.2%	4.4%	5.8%	10.5%	14.3%	16.7%	5.5%	10.7%	12.9%
PIN	3.8%	5.6%	8.0%	5.7%	5.0%	6.8%	13.7%	12.4%	10.4%	5.9%	13.7%	14.0%
MCPI	0.2%	0.0%	0.0%	0.4%	0.2%	0.2%	0.1%	0.1%	0.1%	0.4%	0.4%	0.2%
Lipoxygenase	0.8%	0.8%	1.1%	0.8%	0.7%	0.7%	1.0%	1.2%	1.2%	0.8%	1.4%	1.9%
Other	25.9%	25.5%	26.2%	22.4%	27.4%	26.8%	13.4%	13.1%	13.1%	21.2%	15.2%	18.9%

	Alcalase			Flavourzyme			Neutrase			Trypsin		
Class	0.1%	1%	3%	0.1%	1%	3%	0.1%	1%	3%	0.1%	1%	3%
Patatin	43.4%	45.1%	40.1%	31.4%	41.3%	36.4%	30.8%	27.6%	27.2%	31.6%	18.6%	18.4%
Kunitz_sum	25.8%	22.9%	24.6%	39.1%	25.2%	28.9%	41.1%	45.6%	48.0%	39.9%	50.3%	46.2%
KTI-A	0.2%	0.2%	0.3%	0.7%	0.3%	0.6%	1.2%	1.0%	0.7%	0.5%	0.9%	0.7%
KTI-B	14.0%	11.4%	11.3%	24.3%	14.8%	16.8%	15.9%	16.5%	16.7%	25.5%	21.6%	16.9%
KTI-C	2.3%	3.6%	4.9%	5.0%	3.0%	4.1%	11.8%	12.4%	12.4%	4.5%	15.0%	13.6%
KTI-D	2.3%	1.4%	1.5%	4.0%	2.7%	1.6%	1.7%	1.5%	1.5%	3.9%	2.0%	2.1%
Kunitz_unclassified	6.9%	6.4%	6.7%	5.2%	4.4%	5.8%	10.5%	14.3%	16.7%	5.5%	10.7%	12.9%
PIN	3.8%	5.6%	8.0%	5.7%	5.0%	6.8%	13.7%	12.4%	10.4%	5.9%	13.7%	14.0%
MCPI	0.2%	0.0%	0.0%	0.4%	0.2%	0.2%	0.1%	0.1%	0.1%	0.4%	0.4%	0.2%
Lipoxygenase	0.8%	0.8%	1.1%	0.8%	0.7%	0.7%	1.0%	1.2%	1.2%	0.8%	1.4%	1.9%
Other	25.9%	25.5%	26.2%	22.4%	27.4%	26.8%	13.4%	13.1%	13.1%	21.2%	15.2%	18.9%

Fig 6: Heat map (blue (low) to red (high)) of relative protein abundance (by unspecific I_L^{rel}) according to protein families/classes for all PPHs (freeze-dried supernatant after hydrolysis). Heat map color is normalized by row (top) and column (bottom) for inter- and intra-sample comparison, respectively. All indented Kunitz subclasses (A-D and unclassified) are included in the "Kunitz_sum" abundance, but are listed explicitly to distinguish quantitatively between subclasses.

In the class of "other" protein, which are substantially overrepresented in Alc and Flav PPHs (Fig. 6), the most abundantly quantified proteins (I_L^{rel} > 1% in at least one PPH) are related to stress response and glycolysis/carbohydrate metabolism (Table A.5). These include, for instance, two

induced stolon tip (IST) proteins (P33191 and M1AFN6), which are particularly abundant in the Alc PPHs (6.3-7.7%). Interestingly, the two IST proteins represented <0.005% of the total protein in the same PPI (García-Moreno, Gregersen, et al., 2020), where the PPI was characterized by means of conventional bottom-up proteomics using tryptic in-gel digestion. The two IST proteins constitute <0.7% of the protein in the Tryp PPHs, however only one of 516 peptides identified for P33191 and two of 316 peptides identified for M1AFN6 were fully tryptic (and very low intensity). Consequently, their identification is hence ascribed to the chymotrypsin activity in rTrypsin/PTN (Nongonierma et al., 2017) as the proteins have a very low frequency of tryptic AAs (Arg/Lys). Chymotrypsin activity is absent in pure, sequencing-grade trypsin used for conventional proteomics, explaining the observed discrepancy. In other studies, the two IST proteins were determined to constitute 0.34% of the total protein content in raw potatoes (i.e. not in a isolate/concentrate) (Krutz et al., 2019). Nevertheless, our observations further substantiate how protease specificity and potential selectivity, search parameters, and hydrolysis conditions significantly affect the peptidome of a hydrolysate in a differential manner, as previously reported for bacterial and seaweed protein (Gregersen et al., 2022). This is particularly relevant for short-term, partial enzymatic hydrolysis.

4. Conclusion

In line with increasing focus on green transition and clean label foods, peptides and protein hydrolysates attract significant attention for substituting chemical additives as surface active ingredients in foods. With this work, we present a fundamentally novel approach of data-driven targeted hydrolysis, as an alternative to the conventional trial-and-error methodology. Using prior *in vitro* knowledge of highly potent emulsifier peptides derived from abundant potato proteins, we

use *in silico* sequence analysis to hypothesize that Trypsin can release target peptides through hydrolysis and produce a hydrolysate with superior interfacial activity. This was verified to indeed by true though assessment of emulsifying and foaming properties and by benchmarking against the native substrate, the gold standard (sodium caseinate), an enriched patatin fraction, and a range of industrial proteases. In fact, only the application of Trypsin was able to improve both emulsification activity and stability significantly ($P<0.05$), compared to untreated native substrate. Overall, we found a weak relation between degree of hydrolysis and bulk interfacial activity for the hydrolysates, but DH cannot by itself be used to asses emulsification potential. Using LC-MS/MS analysis, we were able to convert conventional bottom-up proteomics into a non-specific peptidomic analysis, identifying more than 10,000 peptides in each hydrolysate. Using peptide mapping, we show that random overlaps is insufficient for quantitatively describing bulk functionality of hydrolysates, but a deeper, peptide-centric analysis is required. Through this, we show that hydrolysates produced using Trypsin, and to some extent Alcalase, were rich in peptides with much higher amphiphilic potential than the other hydrolysates assayed. Moreover, the 3% tryptic hydrolysate was found to contain predicted peptides, thereby not only validating our novel approach for targeted hydrolysis, but also providing peptide-level evidence to why this particular hydrolysate had the best surface active properties across all hydrolysates investigated. Ultimately, based on modest yields, and that peptides from patatin appear depleted in the hydrolysate, we expect that optimizing process conditions will improve the surface active properties of the tryptic hydrolysate even further. This study further highlights several challenges and bottlenecks related to efficient, large-scale application of the methodology. For instance, a method for accurate and absolute peptide quantification is needed, and better characterization of protease specificity as well as a broader selection of high specificity industrial proteases are prerequisites for further

development in this direction. Nevertheless, this study is yet another example of how interdisciplinary research, big data, and computational predictions is gaining headway in food science and can pave the way for more efficient development in the future while simultaneously providing a deeper fundamental understanding of molecular mechanisms and properties related to food ingredient functionality.

Author contribution

SGE: Conceptualization, Methodology, Formal analysis, Investigation, Validation, Writing – original draft preparation, Writing – review and editing, Visualization, Supervision. AJ: Methodology, Formal analysis, Investigation, Writing – original draft preparation, Writing – review and editing, Visualization. BY: Validation, Writing – review and editing. PJGM: Validation, Writing – review and editing. MGP: Methodology, Formal analysis, Writing – review and editing. DH: Methodology, Formal analysis, Writing – review and editing. CJ: Conceptualization, Writing – review and editing, Funding acquisition, Supervision. MTO: Conceptualization, Methodology, Writing – review and editing, Funding acquisition, Supervision. EBH: Conceptualization, Writing – review and editing, Project administration, Funding acquisition, Supervision.

Acknowledgements

The authors would like to acknowledge KMC AmbA for supplying the potato protein isolate and Lihme Protein Solutions (Denmark) for supplying purified patatin as a reference. Likewise, the

1089 authors would like to acknowledge Arla Foods A/S (Denmark) and Novozymes A/S (Denmark)
1090 for providing sodium caseinate and proteolytic enzymes, respectively.
1091

1092 Funding

1093 This work was supported by Innovation Fund Denmark (Grant number 7045-00021B
1094 (PROVIDE)).
1095

1096 Conflict of interests

1097 The authors declare no conflict of interests.
1098

1099 References

1100 Adjonu, R., Doran, G., Torley, P., & Agboola, S. (2014). Whey protein peptides as components of
1101 nanoemulsions: A review of emulsifying and biological functionalities. *Journal of Food*
1102 *Engineering*, Vol. 122, pp. 15–27. https://doi.org/10.1016/j.jfoodeng.2013.08.034
1103 Adler-Nissen, J. (1986). *Enzymatic hydrolysis of food proteins.* London: Elsevier Applied Science
1104 Publishers.
1105 Akbari, N., Mohammadzadeh Milani, J., & Biparva, P. (2020). Functional and conformational
1106 properties of proteolytic enzyme-modified potato protein isolate. *Journal of the Science of*
1107 *Food and Agriculture*, *100*(3), 1320–1327. https://doi.org/10.1002/jsfa.10148
1108 Aldred, N., Phang, I. Y., Conlan, S. L., Clare, A. S., & Vancso, G. J. (2008). The effects of a serine
1109 protease, Alcalase, on the adhesives of barnacle cyprids (Balanus amphitrite). *Biofouling*,

24(2), 97–107. https://doi.org/10.1080/08927010801885908

Aluko, R. E. (2018). Food protein-derived peptides: Production, isolation, and purification. In *Proteins in Food Processing: Second Edition* (Second Edi, pp. 389–412). https://doi.org/10.1016/B978-0-08-100722-8.00016-4

Bauw, G., Nielsen, H. V., Emmersen, J., Nielsen, K. L., Jørgensen, M., & Welinder, K. G. (2006). Patatins, Kunitz protease inhibitors and other major proteins in tuber of potato cv. Kuras. *FEBS Journal*, *273*(15), 3569–3584. https://doi.org/10.1111/j.1742-4658.2006.05364.x

Bjornshave, A., Johansen, T. N., Amer, B., Dalsgaard, T. K., Holst, J. J., & Hermansen, K. (2019). Pre-meal and postprandial lipaemia in subjects with the metabolic syndrome: effects of timing and protein quality (randomised crossover trial). *British Journal of Nutrition*, *121*(3), 312–321. https://doi.org/10.1017/S0007114518003264

Camire, M. E., Kubow, S., & Donnelly, D. J. (2009). Potatoes and Human Health. *Critical Reviews in Food Science and Nutrition*, *49*(10), 823–840. https://doi.org/10.1080/10408390903041996

Caron, J., Chataigné, G., Gimeno, J. P., Duhal, N., Goossens, J. F., Dhulster, P., … Flahaut, C. (2016). Food peptidomics of in vitro gastrointestinal digestions of partially purified bovine hemoglobin: Low-resolution versus high-resolution LC-MS/MS analyses. *Electrophoresis*, *37*(13), 1814–1822. https://doi.org/10.1002/elps.201500559

Cheng, Y., Liu, Y., Wu, J., Ofori Donkor, P., Li, T., & Ma, H. (2017). Improving the enzymolysis efficiency of potato protein by simultaneous dual-frequency energy-gathered ultrasound pretreatment: Thermodynamics and kinetics. *Ultrasonics Sonochemistry*, *37*, 351–359. https://doi.org/10.1016/j.ultsonch.2017.01.034

Chuang, H.-L., Baskaran, R., Day, C. H., Lin, Y.-M., Ho, C.-C., Ho, T.-J., … Huang, C.-Y. (2020).

Role of potato protein hydrolysate and exercise in preventing high-fat diet-induced hepatocyte apoptosis in senescence-accelerated mouse. *Journal of Food Biochemistry*, *44*(12), e13525. https://doi.org/10.1111/JFBC.13525

Claussen, I. C., Strømmen, I., Egelandsdal, B., & Strætkvern, K. O. (2007). Effects of drying methods on functionality of a native potato protein concentrate. *Drying Technology*, *25*(6), 1091–1098. https://doi.org/10.1080/07373930701396444

Consortium, T. U., Bateman, A., Martin, M.-J., Orchard, S., Magrane, M., Agivetova, R., … Teodoro, D. (2021). UniProt: the universal protein knowledgebase in 2021. *Nucleic Acids Research*, *49*(D1), D480–D489. https://doi.org/10.1093/NAR/GKAA1100

Cox, J., & Mann, M. (2008). MaxQuant enables high peptide identification rates, individualized p.p.b.-range mass accuracies and proteome-wide protein quantification. *Nature Biotechnology*, *26*(12), 1367–1372. https://doi.org/10.1038/nbt.1511

Cui, Q., Sun, Y., Cheng, J., & Guo, M. (2022). Effect of two-step enzymatic hydrolysis on the antioxidant properties and proteomics of hydrolysates of milk protein concentrate. *Food Chemistry*, *366*(July 2021), 130711. https://doi.org/10.1016/j.foodchem.2021.130711

Demirhan, E., Apar, D. K., & Özbek, B. (2011). Sesame cake protein hydrolysis by alcalase: Effects of process parameters on hydrolysis, solubilisation, and enzyme inactivation. *Korean Journal of Chemical Engineering*, *28*(1), 195–202. https://doi.org/10.1007/s11814-010-0316-2

Deng, Y., van der Veer, F., Sforza, S., Gruppen, H., & Wierenga, P. A. (2018). Towards predicting protein hydrolysis by bovine trypsin. *Process Biochemistry*, *65*, 81–92. https://doi.org/10.1016/J.PROCBIO.2017.11.006

Dexter, A. F. (2010). Interfacial and Emulsifying Properties of Designed β-Strand Peptides.

Langmuir, *26*(23), 17997–18007. https://doi.org/10.1021/la103471j

Dexter, A. F., & Middelberg, A. P. J. (2008). Peptides as functional surfactants. *Industrial and Engineering Chemistry Research*, *47*(17), 6391–6398. https://doi.org/10.1021/ie800127f

Donlon, J. (2007). Subtilisin. In J. Polaina & A. P. MacCabe (Eds.), *Industrial Enzymes; Structure, Function and Applications* (pp. 197–206). Springer.

Doucet, D., Otter, D. E., Gauthier, S. F., & Foegeding, E. A. (2003). Enzyme-induced gelation of extensively hydrolyzed whey proteins by alcalase: Peptide identification and determination of enzyme specificity. *Journal of Agricultural and Food Chemistry*, *51*(21), 6300–6308. https://doi.org/10.1021/jf026242v

Du, C., Cai, Y., Liu, T., Huang, L., Long, Z., Zhao, M., … Zhao, Q. (2020). Physicochemical, interfacial and emulsifying properties of insoluble soy peptide aggregate: Effect of homogenization and alkaline-treatment. *Food Hydrocolloids*, *109*(June), 106125. https://doi.org/10.1016/j.foodhyd.2020.106125

Eisenberg, D., Weiss, R. M., & Terwilliger, T. C. (1982). The helical hydrophobic moment: a measure of the amphiphilicity of a helix. *Nature*, *299*(5881), 371–374. https://doi.org/10.1038/299371a0

Elavarasan, K., Naveen Kumar, V., & Shamasundar, B. A. (2014). Antioxidant and functional properties of fish protein hydrolysates from fresh water carp (Catla catla) as influenced by the nature of enzyme. *Journal of Food Processing and Preservation*, *38*(3), 1207–1214. https://doi.org/10.1111/jfpp.12081

Enser, M., Bloomberg, G. B., Brock, C., & Clark, D. C. (1990). De novo design and structure-activity relationships of peptide emulsifiers and foaming agents. *International Journal of Biological Macromolecules*, *12*(2), 118–124. https://doi.org/10.1016/0141-8130(90)90063-

G

Falade, E. O., Mu, T. H., & Zhang, M. (2021). Improvement of ultrasound microwave-assisted enzymatic production and high hydrostatic pressure on emulsifying, rheological and interfacial characteristics of sweet potato protein hydrolysates. *Food Hydrocolloids*, *117*(February), 106684. https://doi.org/10.1016/j.foodhyd.2021.106684

Food and Agriculture Organization of the United Nations. (2020). FAOSTAT Statistical Database.

García-Moreno, P. J., Gregersen, S., Nedamani, E. R., Olsen, T. H., Marcatili, P., Overgaard, M. T., … Jacobsen, C. (2020). Identification of emulsifier potato peptides by bioinformatics: application to omega-3 delivery emulsions and release from potato industry side streams. *Scientific Reports*, *10*(1), 690. https://doi.org/10.1038/s41598-019-57229-6

García-Moreno, P. J., Jacobsen, C., Marcatili, P., Gregersen, S., Overgaard, M. T., Andersen, M. L., … Hansen, E. B. (2020). Emulsifying peptides from potato protein predicted by bioinformatics: Stabilization of fish oil-in-water emulsions. *Food Hydrocolloids*, *101*, 105529. https://doi.org/10.1016/j.foodhyd.2019.105529

García-Moreno, P. J., Stephansen, K., Van Der Kruijs, J., Guadix, A., Guadix, E. M., Chronakis, I. S., & Jacobsen, C. (2016). Encapsulation of fish oil in nanofibers by emulsion electrospinning: Physical characterization and oxidative stability. *Journal of Food Engineering*, *183*, 39–49. https://doi.org/10.1016/j.jfoodeng.2016.03.015

García-Moreno, P. J., Yang, J., Gregersen, S., Jones, N. C., Berton-Carabin, C. C., Sagis, L. M. C., … Jacobsen, C. (2021). The structure, viscoelasticity and charge of potato peptides adsorbed at the oil-water interface determine the physicochemical stability of fish oil-in-water emulsions. *Food Hydrocolloids*, *115*, 106605. Retrieved from https://linkinghub.elsevier.com/retrieve/pii/S0268005X21000217

García Arteaga, V., Apéstegui Guardia, M., Muranyi, I., Eisner, P., & Schweiggert-Weisz, U. (2020). Effect of enzymatic hydrolysis on molecular weight distribution, techno-functional properties and sensory perception of pea protein isolates. *Innovative Food Science & Emerging Technologies*, *65*, 102449. https://doi.org/10.1016/J.IFSET.2020.102449

Giansanti, P., Tsiatsiani, L., Low, T. Y., & Heck, A. J. R. (2016). Six alternative proteases for mass spectrometry-based proteomics beyond trypsin. *Nature Protocols*, *11*(5), 993–1006. https://doi.org/10.1038/nprot.2016.057

Gregersen, S., Kongsted, A.-S. H., Nielsen, R. B., Hansen, S. S., Lau, F. A., Rasmussen, J. B., … Jacobsen, C. (2021). Enzymatic extraction improves intracellular protein recovery from the industrial carrageenan seaweed Eucheuma denticulatum revealed by quantitative, subcellular protein profiling: A high potential source of functional food ingredients. *Food Chemistry: X*, *12*, 100137. https://doi.org/10.1016/J.FOCHX.2021.100137

Gregersen, S., Pertseva, M., Marcatili, P., Holdt, S. L., Jacobsen, C., Garcia-Moreno, P. J., … Overgaard, M. T. (2022). Proteomic characterization of pilot scale hot-water extracts from the industrial carrageenan red seaweed Eucheuma denticulatum. *Algal Research*, *62*, 102619. https://doi.org/10.1016/J.ALGAL.2021.102619

Hanley, J., & James, T. (2018). Synthesis, chemistry, physicochemical properties and industrial applications of amino acid surfactants : A review. *Comptes Rendus Chimie*, 112–130. https://doi.org/10.1016/j.crci.2017.11.005

Hashemi, A., & Jafarpour, A. (2016). Rheological and microstructural properties of beef sausage batter formulated with fish fillet mince. *Journal of Food Science and Technology*, *53*(1), 601–610. https://doi.org/10.1007/s13197-015-2052-4

Heibges, A., Glaczinski, H., Ballvora, A., Salamini, F., & Gebhardt, C. (2003). Structural diversity

and organization of three gene families for Kunitz-type enzyme inhibitors from potato tubers (Solanum tuberosum l.). *Molecular Genetics and Genomics*, *269*(4), 526–534. https://doi.org/10.1007/s00438-003-0860-0

Hinnenkamp, C., & Ismail, B. P. (2021). A proteomics approach to characterizing limited hydrolysis of whey protein concentrate. *Food Chemistry*, *350*(February), 129235. https://doi.org/10.1016/j.foodchem.2021.129235

Huang, D. Y., Swanson, B. G., & Ryan, C. A. (1981). Stability of Proteinase Inhibitors in Potato Tubers During Cooking. *Journal of Food Science*, *46*(1), 287–290. https://doi.org/https://doi.org/10.1111/j.1365-2621.1981.tb14583.x

Huang, Y. P., Dias, F. F. G., Leite Nobrega de Moura Bell, J. M., & Barile, D. (2022). A complete workflow for discovering small bioactive peptides in foods by LC-MS/MS: A case study on almonds. *Food Chemistry*, *369*, 130834. https://doi.org/10.1016/j.foodchem.2021.130834

Jafarpour, A., Gomes, R. M., Gregersen, S., Sloth, J. J., Jacobsen, C., & Moltke Sørensen, A. D. (2020). Characterization of cod (Gadus morhua) frame composition and its valorization by enzymatic hydrolysis. *Journal of Food Composition and Analysis*, *89*, 103469. https://doi.org/10.1016/j.jfca.2020.103469

Jafarpour, A., Gregersen, S., Marciel Gomes, R., Marcatili, P., Hegelund Olsen, T., Jacobsen, C., … Sørensen, A.-D. M. (2020). Biofunctionality of Enzymatically Derived Peptides from Codfish (Gadus morhua) Frame: Bulk In Vitro Properties, Quantitative Proteomics, and Bioinformatic Prediction. *Marine Drugs*, *18*(12), 599. https://doi.org/10.3390/md18120599

Jarnuczak, A. F., Lee, D. C. H., Lawless, C., Holman, S. W., Eyers, C. E., & Hubbard, S. J. (2016). Analysis of Intrinsic Peptide Detectability via Integrated Label-Free and SRM-Based Absolute Quantitative Proteomics. *Journal of Proteome Research*, *15*(9), 2945–2959.

https://doi.org/10.1021/acs.jproteome.6b00048

Jin, Y., Yan, J., Yu, Y., & Qi, Y. (2015). Screening and identification of DPP-IV inhibitory peptides from deer skin hydrolysates by an integrated approach of LC-MS/MS and in silico analysis. *Journal of Functional Foods*, *18*, 344–357. https://doi.org/10.1016/j.jff.2015.07.015

Jones, D. B. (1931). Factors for Converting Percentages of Nitrogen in Foods and Feeds Into percentages of protein.

Jørgensen, M., Bauw, G., & Welinder, K. G. (2006). Molecular properties and activities of tuber proteins from starch potato cv. Kuras. *Journal of Agricultural and Food Chemistry*, *54*(25), 9389–9397. https://doi.org/10.1021/jf0623945

Jørgensen, M., Stensballe, A., & Welinder, K. G. (2011). Extensive post-translational processing of potato tuber storage proteins and vacuolar targeting. *FEBS Journal*, *278*(21), 4070–4087. https://doi.org/10.1111/j.1742-4658.2011.08311.x

Kamnerdpetch, C., Weiss, M., Kasper, C., & Scheper, T. (2007). An improvement of potato pulp protein hydrolyzation process by the combination of protease enzyme systems. *Enzyme and Microbial Technology*, *40*(4), 508–514. https://doi.org/10.1016/j.enzmictec.2006.05.006

Karami, Z., & Akbari-adergani, B. (2019). Bioactive food derived peptides: a review on correlation between structure of bioactive peptides and their functional properties. *Journal of Food Science and Technology*, *56*(2), 535–547. https://doi.org/10.1007/s13197-018-3549-4

Kärenlampi, S. O., & White, P. J. (2009). Potato Proteins, Lipids, and Minerals. In *Advances in Potato Chemistry and Technology* (pp. 99–125). https://doi.org/10.1016/b978-0-12-374349-7.00005-2

Keppler, J. K., Schwarz, K., & van der Goot, A. J. (2020). Covalent modification of food proteins by plant-based ingredients (polyphenols and organosulphur compounds): A commonplace

reaction with novel utilization potential. *Trends in Food Science and Technology*, *101*, 38–49. https://doi.org/10.1016/j.tifs.2020.04.023

Klompong, V., Benjakul, S., Kantachote, D., & Shahidi, F. (2007). Antioxidative activity and functional properties of protein hydrolysate of yellow stripe trevally (Selaroides leptolepis) as influenced by the degree of hydrolysis and enzyme type. *Food Chemistry*, *102*(4), 1317–1327. https://doi.org/10.1016/j.foodchem.2006.07.016

Krutz, N. L., Winget, J., Ryan, C. A., Wimalasena, R., Maurer-Stroh, S., Dearman, R. J., … Gerberick, G. F. (2019). Proteomic and Bioinformatic Analyses for the Identification of Proteins with Low Allergenic Potential for Hazard Assessment. *Toxicological Sciences*, *170*(1), 210–222. https://doi.org/10.1093/toxsci/kfz078

Kurozawa, L. E., Morassi, A. G., Vanzo, A. A., Park, K. J., & Hubinger, M. D. (2009). Influence of spray drying conditions on physicochemical properties of chicken meat powder. *Drying Technology*, *27*(11), 1248–1257. https://doi.org/10.1080/07373930903267187

Lacou, L., Léonil, J., & Gagnaire, V. (2016, June 1). Functional properties of peptides: From single peptide solutions to a mixture of peptides in food products. *Food Hydrocolloids*, Vol. 57, pp. 187–199. https://doi.org/10.1016/j.foodhyd.2016.01.028

Le Guenic, S., Chaveriat, L., Lequart, V., Joly, N., & Martin, P. (2019). Renewable Surfactants for Biochemical Applications and Nanotechnology. *Journal of Surfactants and Detergents*, *22*(1), 5–21. https://doi.org/10.1002/jsde.12216

Lei, F., Cui, C., Zhao, Q., Sun-Waterhouse, D., & Zhao, M. (2014). Evaluation of the Hydrolysis Specificity of Protease from Marine Exiguobacterium sp. SWJS2 via Free Amino Acid Analysis. *Applied Biochemistry and Biotechnology*, *174*(4), 1260–1271. https://doi.org/10.1007/s12010-014-1088-7

1294 Li-Chan, E. C. Y. (2015, February 1). Bioactive peptides and protein hydrolysates: Research trends
1295 and challenges for application as nutraceuticals and functional food ingredients. *Current*
1296 *Opinion in Food Science*, Vol. 1, pp. 28–37. https://doi.org/10.1016/j.cofs.2014.09.005
1297 Li, M., Zheng, H., Lin, M., Zhu, W., & Zhang, J. (2020). Characterization of the protein and
1298 peptide of excipient zein by the multi-enzyme digestion coupled with nano-LC-MS/MS. *Food*
1299 *Chemistry*, *321*(October 2019), 126712. https://doi.org/10.1016/j.foodchem.2020.126712
1300 Li, X., Deng, J., Shen, S., Li, T., Yuan, M., Yang, R., & Ding, C. (2015). Antioxidant activities
1301 and functional properties of enzymatic protein hydrolysates from defatted Camellia oleifera
1302 seed cake. *Journal of Food Science and Technology*, *52*(9), 5681–5690.
1303 https://doi.org/10.1007/s13197-014-1693-z
1304 Liang, G., Chen, W., Qie, X., Zeng, M., Qin, F., He, Z., & Chen, J. (2020). Modification of soy
1305 protein isolates using combined pre-heat treatment and controlled enzymatic hydrolysis for
1306 improving foaming properties. *Food Hydrocolloids*, *105*(May 2019), 105764.
1307 https://doi.org/10.1016/j.foodhyd.2020.105764
1308 Linderstrøm-Lang, K. (1953). The initial phases of the enzymatic degradation of proteins. *Bulletin*
1309 *de la Societe de chimie biologique*, *35*(1–2), 100–116.
1310 Liska, D. J., Cook, C. M., Wang, D. D., & Szpylka, J. (2016). Maillard reaction products and
1311 potatoes: have the benefits been clearly assessed? *Food Science & Nutrition*, *4*(2), 234–249.
1312 https://doi.org/10.1002/fsn3.283
1313 Liu, Q., Kong, B., Xiong, Y. L., & Xia, X. (2010). Antioxidant activity and functional properties
1314 of porcine plasma protein hydrolysate as influenced by the degree of hydrolysis. *Food*
1315 *Chemistry*, *118*(2), 403–410. https://doi.org/10.1016/j.foodchem.2009.05.013
1316 Løkra, S., & Strætkvern, K. O. (2009). Industrial Proteins from Potato Juice. A Review. *Food*,

3(1), 88–95.

Lu, X., Sun, Q., Zhang, L., Wang, R., Gao, J., Jia, C., & Huang, J. (2021). Dual-enzyme hydrolysis for preparation of ACE-inhibitory peptides from sesame seed protein: Optimization, separation, and identification. *Journal of Food Biochemistry*, *45*(4), 1–18. https://doi.org/10.1111/jfbc.13638

Mao, C., Wu, J., Zhang, X., Ma, F., & Cheng, Y. (2020). Improving the Solubility and Digestibility of Potato Protein with an Online Ultrasound-Assisted PH Shifting Treatment at Medium Temperature. *Foods 2020, Vol. 9, Page 1908*, *9*(12), 1908. https://doi.org/10.3390/FOODS9121908

Mariotti, F., Tomé, D., & Mirand, P. P. (2008). Converting Nitrogen into Protein—Beyond 6.25 and Jones' Factors. *Critical Reviews in Food Science and Nutrition*, *48*(2), 177–184. https://doi.org/10.1080/10408390701279749

McClements, D. J., & Jafari, S. M. (2018). Improving emulsion formation, stability and performance using mixed emulsifiers: A review. *Advances in Colloid and Interface Science*, *251*, 55–79. https://doi.org/10.1016/j.cis.2017.12.001

Miedzianka, J., Pęksa, A., Pokora, M., Rytel, E., Tajner-Czopek, A., & Kita, A. (2014). Improving the properties of fodder potato protein concentrate by enzymatic hydrolysis. *Food Chemistry*, *159*, 512–518. https://doi.org/10.1016/j.foodchem.2014.03.054

Mondal, S., Varenik, M., Bloch, D. N., Atsmon-Raz, Y., Jacoby, G., Adler-Abramovich, L., … Gazit, E. (2017). A minimal length rigid helical peptide motif allows rational design of modular surfactants. *Nature Communications*, *8*. https://doi.org/10.1038/ncomms14018

Moreno, M. C. M., Cuadrado, V. F., Marquez Moreno, M. C., & Fernandez Cuadrado, V. (1993). Enzymic hydrolysis of vegetable proteins: mechanism and kinetics. *Process Biochemistry*,

28(7), 481–490. https://doi.org/10.1016/0032-9592(93)85032-B

Nakai, S., Alizadeh-Pasdar, N., Dou, J., Buttimor, R., Rousseau, D., & Paulson, A. (2004). Pattern Similarity Analysis of Amino Acid Sequences for Peptide Emulsification. *Journal of Agricultural and Food Chemistry*, *52*(4), 927–934. https://doi.org/10.1021/jf034744i

Nisov, A., Ercili-Cura, D., & Nordlund, E. (2020). Limited hydrolysis of rice endosperm protein for improved techno-functional properties. *Food Chemistry*, *302*(February 2019), 125274. https://doi.org/10.1016/j.foodchem.2019.125274

Nongonierma, A. B., Paolella, S., Mudgil, P., Maqsood, S., & FitzGerald, R. J. (2017). Dipeptidyl peptidase IV (DPP-IV) inhibitory properties of camel milk protein hydrolysates generated with trypsin. *Journal of Functional Foods*, *34*, 49–58. https://doi.org/10.1016/j.jff.2017.04.016

O'Keeffe, M. B., & FitzGerald, R. J. (2014). Antioxidant effects of enzymatic hydrolysates of whey protein concentrate on cultured human endothelial cells. *International Dairy Journal*, *36*(2), 128–135. https://doi.org/10.1016/j.idairyj.2014.01.013

Padial-Domínguez, M., Espejo-Carpio, F. J., Pérez-Gálvez, R., Guadix, A., & Guadix, E. M. (2020). Optimization of the Emulsifying Properties of Food Protein Hydrolysates for the Production of Fish Oil-in-Water Emulsions. *Foods*, *9*(5), 636. https://doi.org/10.3390/foods9050636

Pearce, K. N., & Kinsella, J. E. (1978). Emulsifying Properties of Proteins: Evaluation of a Turbidimetric Technique. *Journal of Agricultural and Food Chemistry*, *26*(3), 716–723. https://doi.org/10.1021/jf60217a041

Pęksa, A., & Miedzianka, J. (2014). Amino acid composition of enzymatically hydrolysed potato protein preparations. *Czech Journal of Food Sciences*, *32*(3), 265–272.

https://doi.org/10.17221/286/2013-cjfs

Pęksa, A., & Miedzianka, J. (2021). Potato industry by-products as a source of protein with beneficial nutritional, functional, health-promoting and antimicrobial properties. *Applied Sciences (Switzerland)*, *11*(8). https://doi.org/10.3390/app11083497

Petruccelli, S., & Anon, M. C. (1995). Soy Protein Isolate Components and Their Interactions. *J. Agric. Food Chem*, *43*(7), 1762–1767. https://doi.org/10.1021/jf00055a004

Peyronel, D. V., & Cantera, A. M. B. (1995). A simple and rapid technique for postelectrophoretic detection of proteases using azocasein. *Electrophoresis*, *16*(1), 1894–1897. https://doi.org/10.1002/elps.11501601311

Pouvreau, L., Gruppen, H., Piersma, S. R. R., van den Broek, L. A. A. M., Van Koningsveld, G. A. A., & Voragen, A. . G. J. (2001). Relative Abundance and Inhibitory Distribution of Protease Inhibitors in Potato Juice from cv. Elkana. *Journal of Agricultural and Food Chemistry*, *49*(6), 2864–2874. https://doi.org/10.1021/jf010126v

Rabe, S., Fischer, L., Blank, I., Berends, P., Appel, D., Eisele, T., … Merz, M. (2015). Flavourzyme, an Enzyme Preparation with Industrial Relevance: Automated Nine-Step Purification and Partial Characterization of Eight Enzymes. *Journal of Agricultural and Food Chemistry*, *63*(23), 5682–5693. https://doi.org/10.1021/acs.jafc.5b01665

Ralet, M. C., & Guéguen, J. (2000). Fractionation of Potato Proteins: Solubility, Thermal Coagulation and Emulsifying Properties. *LWT - Food Science and Technology*, *33*(5), 380–387. https://doi.org/10.1006/fstl.2000.0672

Refstie, S., & Tiekstra, H. A. J. (2003). Potato protein concentrate with low content of solanidine glycoalkaloids in diets for Atlantic salmon (Salmo salar). *Aquaculture*, *216*(1–4), 283–298. https://doi.org/10.1016/S0044-8486(02)00434-9

1386 Ricardo, F., Pradilla, D., Cruz, J. C., & Alvarez, O. (2021). Emerging Emulsifiers: Conceptual
1387 Basis for the Identification and Rational Design of Peptides with Surface Activity.
1388 *International Journal of Molecular Sciences*, *22*(9), 4615.
1389 https://doi.org/10.3390/ijms22094615
1390 Rodan, K., Fields, K., & Falla, T. (2013). Bioactive Peptides. *Cosmeceuticals and Cosmetic*
1391 *Practice*, 142–152. https://doi.org/10.1002/9781118384824.ch14
1392 Rodríguez-Díaz, J. C., Tonon, R. V., & Hubinger, M. D. (2014). Spray Drying of Blue Shark Skin
1393 Protein Hydrolysate: Physical, Morphological, and Antioxidant Properties. *Drying*
1394 *Technology*, *32*(16), 1986–1996. https://doi.org/10.1080/07373937.2014.928726
1395 Saito, M., Ogasawara, M., Chikuni, K., & Shimizu, M. (1995). Synthesis of a Peptide Emulsifier
1396 with an Amphiphilic Structure. *Bioscience, Biotechnology and Biochemistry*, *59*(3), 388–392.
1397 https://doi.org/10.1271/bbb.59.388
1398 Sapers, G. M., & Miller, R. L. (1992). Enzymatic browning control in potato with ascorbic acid-
1399 2-phosphates. *Journal of Food Science*, *57*(5), 1132–1135. https://doi.org/10.1111/j.1365-
1400 2621.1992.tb11281.x
1401 Sarabandi, K., Sadeghi Mahoonak, A., Hamishekar, H., Ghorbani, M., & Jafari, S. M. (2018).
1402 Microencapsulation of casein hydrolysates: Physicochemical, antioxidant and microstructure
1403 properties. *Journal of Food Engineering*, *237*(March), 86–95.
1404 https://doi.org/10.1016/j.jfoodeng.2018.05.036
1405 Sbroggio, M. F., Montilha, M. S., Figueiredo, V. R. G. de, Georgetti, S. R., & Kurozawa, L. E.
1406 (2016). Influence of the degree of hydrolysis and type of enzyme on antioxidant activity of
1407 okara protein hydrolysates. *Food Science and Technology*, *36*(2), 375–381.
1408 https://doi.org/10.1590/1678-457X.000216

1409 Schmidt, J. M., Damgaard, H., Greve-Poulsen, M., Sunds, A. V., Larsen, L. B., & Hammershøj,
1410 M. (2019). Gel properties of potato protein and the isolated fractions of patatins and protease
1411 inhibitors – Impact of drying method, protein concentration, pH and ionic strength. *Food*
1412 *Hydrocolloids*, *96*, 246–258. https://doi.org/10.1016/j.foodhyd.2019.05.022
1413 Schwanhüusser, B., Busse, D., Li, N., Dittmar, G., Schuchhardt, J., Wolf, J., … Selbach, M.
1414 (2011). Global quantification of mammalian gene expression control. *Nature*, *473*(7347),
1415 337–342. https://doi.org/10.1038/nature10098
1416 Siebert, K. J. (2001). Quantitative structure-activity relationship modeling of peptide and protein
1417 behavior as a function of amino acid composition. *Journal of Agricultural and Food*
1418 *Chemistry*, *49*(2), 851–858. https://doi.org/10.1021/jf000718y
1419 Sievers, F., Wilm, A., Dineen, D., Gibson, T. J., Karplus, K., Li, W., … Higgins, D. G. (2011).
1420 Fast, scalable generation of high-quality protein multiple sequence alignments using Clustal
1421 Omega. *Molecular Systems Biology*, *7*(539). https://doi.org/10.1038/msb.2011.75
1422 Sinitcyn, P., Rudolph, J. D., & Cox, J. (2018). Computational Methods for Understanding Mass
1423 Spectrometry–Based Shotgun Proteomics Data. *Annual Review of Biomedical Data Science*,
1424 *1*(1), 207–234. https://doi.org/10.1146/annurev-biodatasci-080917-013516
1425 Taherian, A. R., Britten, M., Sabik, H., & Fustier, P. (2011). Ability of whey protein isolate and/or
1426 fish gelatin to inhibit physical separation and lipid oxidation in fish oil-in-water beverage
1427 emulsion. *Food Hydrocolloids*, *25*(5), 868–878.
1428 https://doi.org/10.1016/j.foodhyd.2010.08.007
1429 Tamm, F., Gies, K., Diekmann, S., Serfert, Y., Strunskus, T., Brodkorb, A., & Drusch, S. (2015).
1430 Whey protein hydrolysates reduce autoxidation in microencapsulated long chain
1431 polyunsaturated fatty acids. *European Journal of Lipid Science and Technology*, *117*(12),

1960–1970. https://doi.org/10.1002/ejlt.201400574

Thiansilakul, Y., Benjakul, S., & Shahidi, F. (2007). Compositions, functional properties and antioxidative activity of protein hydrolysates prepared from round scad (Decapterus maruadsi). *Food Chemistry*, *103*(4), 1385–1394. https://doi.org/10.1016/J.FOODCHEM.2006.10.055

Tien, C. LE, Vachon, C., Mateescu, M.-A., & Lacroix, M. (2001). Milk protein coatings prevent oxidative browning of apples and potatoes. *Journal of Food Science*, *66*(4), 512–516. https://doi.org/10.1111/j.1365-2621.2001.tb04594.x

Tyanova, S., Temu, T., & Cox, J. (2016). The MaxQuant computational platform for mass spectrometry-based shotgun proteomics. *Nature Protocols*, *11*(12), 2301–2319. https://doi.org/10.1038/nprot.2016.136

Van Koningsveld, G. A., Gruppen, H., De Jongh, H. H. J., Wijngaards, G., Van Boekel, M. A. J. S., Walstra, P., & Voragen, A. G. J. (2001). Effects of pH and heat treatments on the structure and solubility of potato proteins in different preparations. *Journal of Agricultural and Food Chemistry*, *49*(10), 4889–4897. https://doi.org/10.1021/jf010340j

Van Koningsveld, G. A., Walstra, P., Voragen, A. G. J. J., Kuijpers, I. J., Van Boekel, M. A. J. S. J. S., & Gruppen, H. (2006). Effects of Protein Composition and Enzymatic Activity on Formation and Properties of Potato Protein Stabilized Emulsions. *Journal of Agricultural and Food Chemistry*, *54*(17), 6419–6427. https://doi.org/10.1021/jf061278z

Vioque, J., Sánchez-vioque, R., Clemente, A., Pedroche, J., & Millán, F. (2000). Partially Hydrolyzed Rapeseed Protein Isolates with Improved Functional Properties. *Water*, (4), 447–450. https://doi.org/10.1007/s11746-000-0072-y

Waglay, A., & Karboune, S. (2016a). Enzymatic generation of peptides from potato proteins by

selected proteases and characterization of their structural properties. *Biotechnology Progress*, *32*(2), 420–429. https://doi.org/10.1002/btpr.2245

Waglay, A., & Karboune, S. (2016b). Potato Proteins: Functional Food Ingredients. In *Advances in Potato Chemistry and Technology: Second Edition* (Second Edi, pp. 75–104). https://doi.org/10.1016/B978-0-12-800002-1.00004-2

Wang, L. L., & Xiong, Y. L. (2005). Inhibition of Lipid Oxidation in Cooked Beef Patties by Hydrolyzed Potato Protein Is Related to Its Reducing and Radical Scavenging Ability. *Journal of Agricultural and Food Chemistry*, *53*(23). https://doi.org/10.1021/jf051213g

Wouters, A. G. B., Rombouts, I., Fierens, E., Brijs, K., & Delcour, J. A. (2016). Relevance of the Functional Properties of Enzymatic Plant Protein Hydrolysates in Food Systems. *Comprehensive Reviews in Food Science and Food Safety*, *15*(4), 786–800. https://doi.org/10.1111/1541-4337.12209

Wu, J. W., & Chen, X. L. (2011). Extracellular metalloproteases from bacteria. *Applied Microbiology and Biotechnology*, *92*(2), 253–262. https://doi.org/10.1007/s00253-011-3532-8

Wychowaniec, J. K., Patel, R., Leach, J., Mathomes, R., Chhabria, V., Patil-Sen, Y., … Elsawy, M. A. (2020). Aromatic Stacking Facilitated Self-Assembly of Ultrashort Ionic Complementary Peptide Sequence: β-Sheet Nanofibers with Remarkable Gelation and Interfacial Properties. *Biomacromolecules*, *21*(7), 2670–2680. https://doi.org/10.1021/acs.biomac.0c00366

Yesiltas, B., Gregersen, S., Lægsgaard, L., Brinch, M. L., Olsen, T. H., Marcatili, P., … García-Moreno, P. J. (2021). Emulsifier peptides derived from seaweed, methanotrophic bacteria, and potato proteins identified by quantitative proteomics and bioinformatics. *Food*

Chemistry, *362*, 130217. https://doi.org/10.1016/J.FOODCHEM.2021.130217

Zhao, Q., Xiong, H., Selomulya, C., Chen, X. D., Zhong, H., Wang, S., … Zhou, Q. (2012). Enzymatic hydrolysis of rice dreg protein: Effects of enzyme type on the functional properties and antioxidant activities of recovered proteins. *Food Chemistry*, *134*(3), 1360–1367. https://doi.org/10.1016/j.foodchem.2012.03.033

Zhao, X., & Hou, Y. (2009). Limited hydrolysis of soybean protein concentrate and isolate with two proteases and the impact on emulsifying activity index of hydrolysates. *African Journal of Biotechnology*, *8*(14), 3314–3319. https://doi.org/10.5897/AJB09.262